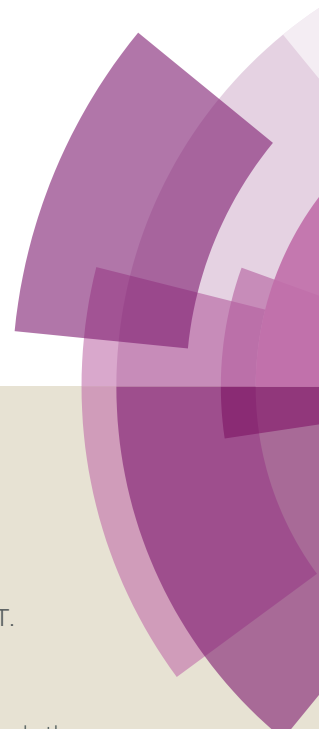
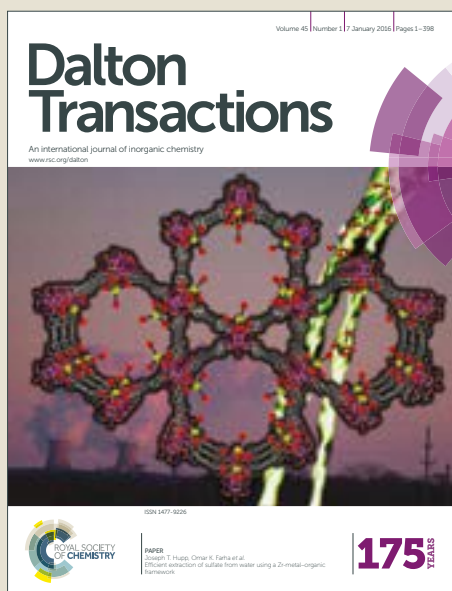


Dalton Transactions

Accepted Manuscript



This article can be cited before page numbers have been issued, to do this please use: C. Nakonkhet, T. Nanok, W. Wattanathana, P. Chuawong and P. Hormnirun, *Dalton Trans.*, 2017, DOI: 10.1039/C7DT02435E.



This is an Accepted Manuscript, which has been through the Royal Society of Chemistry peer review process and has been accepted for publication.

Accepted Manuscripts are published online shortly after acceptance, before technical editing, formatting and proof reading. Using this free service, authors can make their results available to the community, in citable form, before we publish the edited article. We will replace this Accepted Manuscript with the edited and formatted Advance Article as soon as it is available.

You can find more information about Accepted Manuscripts in the [author guidelines](#).

Please note that technical editing may introduce minor changes to the text and/or graphics, which may alter content. The journal's standard [Terms & Conditions](#) and the ethical guidelines, outlined in our [author and reviewer resource centre](#), still apply. In no event shall the Royal Society of Chemistry be held responsible for any errors or omissions in this Accepted Manuscript or any consequences arising from the use of any information it contains.

Aluminium complexes containing salicylbenzothiazole ligands and their application in the ring-opening polymerisation of *rac*-lactide and ϵ -caprolactone

Chutikan Nakonkhet,^a Tanin Nanok,^b Worawat Wattanathana,^c Pitak Chuawong^d and Pimpa Hormnirun^{*,a}

^aLaboratory of Catalysts and Advanced Polymer Materials, Department of Chemistry and Center of Excellence for Innovation in Chemistry, Faculty of Science, Kasetsart University, Bangkok 10900, Thailand

^bDepartment of Chemistry, Faculty of Science, Kasetsart University, Bangkok 10900, Thailand

^cDepartment of Materials Engineering, Faculty of Engineering, Kasetsart University, Bangkok 10900, Thailand.

^dDepartment of Chemistry and Center of Excellence for Innovation in Chemistry, Faculty of Science, and Special Research Unit for Advanced Magnetic Resonance (AMR), Kasetsart University, Bangkok 10900, Thailand

*E-mail: fscipph@ku.ac.th

†Electronic supplementary information (ESI available): ¹H NMR spectra of complexes **1a–7a** and **1b–7b**, crystallographic data and structure refinement details for complexes **5a** and **1b**, polymerisation data and DFT calculation data. See DOI:10.1039/x0xx00000x

ABSTRACT

Two series of aluminium complexes bearing salicylbenzothiazole ligands, four-coordinate aluminium complexes (**1a–7a**) and five-coordinate aluminium complexes (**1b–7b**), were synthesized and characterized by NMR spectroscopy, elemental analysis and X-ray diffraction crystallography (for **5a** and **1b**). Their application for the ring-opening polymerisation of *rac*-lactide and ϵ -caprolactone was studied with the aim of drawing comparisons to closely related aluminium salicylbenzoxazole complexes previously investigated. In the presence of benzyl alcohol, all complexes were active initiators and the polymerisations were all well-controlled and living. Kinetic studies revealed first-order

kinetics in the monomer. In comparison, the catalytic activity of aluminium salicylbenzothiazole complexes was lower than that of aluminium salicylbenzoxazole counterparts. Detailed DFT calculations were performed and indicated that the observed lower catalytic activity of aluminium salicylbenzothiazole complexes agreed well with the observed higher Gibbs free energy at the ring-opening transition state.

INTRODUCTION

Polylactide (PLA) is one of the most important synthetic polyesters due to its biodegradability, biocompatibility and biorenewability.¹⁻³ In general, high molecular weight PLA can be obtained by three different methods: (a) direct condensation polymerisation; (b) azeotropic dehydrative condensation and (c) ring-opening polymerisation (ROP) through lactide formation.⁴ Nonetheless, the ring-opening polymerisation catalyzed by discrete metal complexes stabilized by various ligand architectures is the most effective method to control polymer microstructure. In the case of the *racemic* mixture of L-LA and D-LA or *rac*-LA, the ROP can lead to different chain microstructures, *i.e.* atactic, heterotactic, stereoblock or stereocomplex PLA.^{5,6} Since the physical, mechanical and degradable properties of PLA are correlated to the polymer chain microstructure, research into the stereocontrolled ROP of *rac*-LA has thus received continuous interest over the past few decades as exemplified by large amount of literature in this field.⁷⁻¹⁴

To access the excellent stereocontrol, various metal complexes of Al,¹⁵⁻¹⁹ Ga,^{20,21} Zn,²²⁻²⁴ Mg,^{25,26} In,²⁷⁻²⁹ and other transition metals³⁰⁻³² have been investigated as catalysts/initiators for the ROP of *rac*-LA. However, among the variety of metal complexes, aluminium-based catalysts have shown significant stereocontrol in the ROP of *rac*-LA.³³ In particular, aluminium complexes bearing tetradentate dianionic ligands, such as salen,³⁴⁻³⁷ salan,³⁸⁻⁴³ and salalen,⁴³⁻⁴⁷ displayed by far a remarkable stereocontrol of the polymer

microstructure. The highly isotactic PLA or highly heterotactic PLA can be successfully synthesized.^{35,38,42} On the contrary, the exploitation of aluminium complexes containing bidentate monoanionic ligands, such as phenoxy-imine,⁴⁸⁻⁵² phenoxy-amine,^{53,54} β -diketiminato,⁵⁵⁻⁵⁸ amidinate,⁵⁹ and pyrrolylaldiminate,^{60,61} exhibited a lower degree of stereocontrol due to the limited influence of steric hindrance by the lack of backbone linkers. Furthermore, aluminium complexes with various bidentate monoanionic ligands have also been reported as active initiators for the ROP of ϵ -caprolactone.^{48-50,55,62-68} The effect of ligand structure was found to have a strong influence on the catalytic activity. Recently, the activity rating of different discrete metal based catalytic systems was reviewed and a new way of classifying catalyst activity to enable easier comparisons between literature reports was introduced by Redshaw *et al.*⁶⁹ Since the nature and structure of ancillary ligands used play an important role in the catalytic activity of a catalyst, the search for stereoselective metal complexes of chelating bidentate ligands still remains a great challenge in this field.

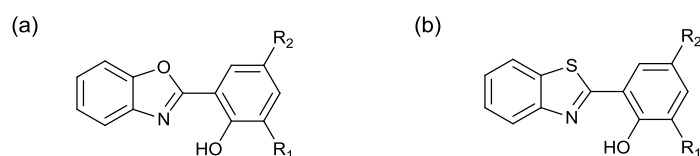


Fig. 1. Structures of (a) salicylbenzoxazole (previous work) and (b) salicylbenzothiazole ligands (this work).

Recently, we have developed aluminium complexes bearing salicylbenzoxazole ligands (Fig.1a) as initiators for the ROP of *rac*-LA and ϵ -CL.⁷⁰ The polymerisations were well-controlled and a good isoselectivity control with the highest P_m value of 0.75 was achieved. Recently, investigations of the effect of O/S exchange in ligand structure of various catalyst systems on the Lewis acidity of the metal center with intriguing influence on the

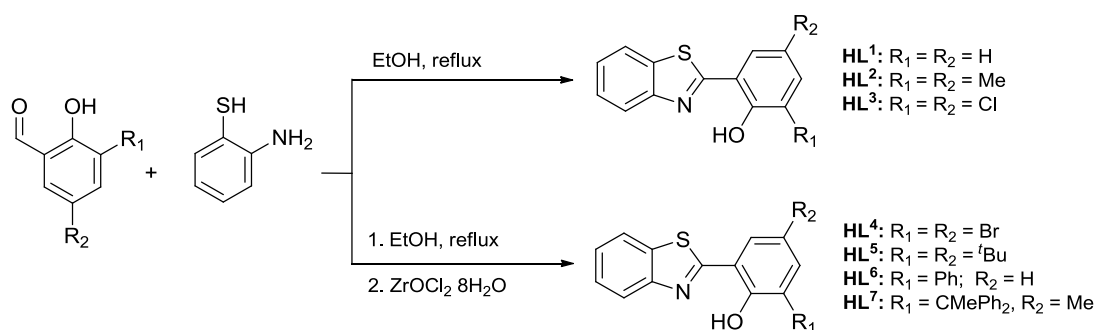
catalytic activity were reported.⁷¹⁻⁷⁴ For example, aluminium complexes bearing N,S-Schiff base ligands showed significantly higher polymerisation rate than aluminium complexes containing N,O-Schiff base ligands in both ϵ -CL and *L*-LA polymerisations.⁷³ Herein, we report the synthesis of salicylbenzothiazole ligands which are sulfur analogs of the salicylbenzoxazole ligands (Fig. 1b),⁷⁵ the coordination of these ligands to the aluminium metal, and the ROP studies of *rac*-LA and ϵ -CL. To the best of our knowledge, this is the first report on the use of aluminium salicylbenzothiazole complexes for the application in the ROP of cyclic esters. Furthermore, the mechanistic insights into the ROP processes employing aluminium salicylbenzothiazole and aluminium salicylbenzoxazole complexes were revealed by density functional theory (DFT) calculations.

RESULTS AND DISCUSSION

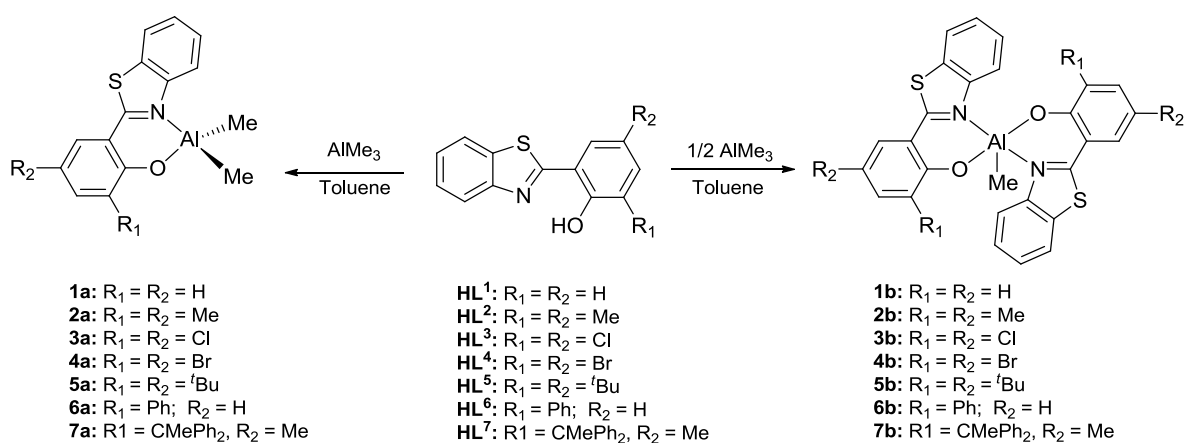
Synthesis and characterization of aluminium complexes 1a–7a and 1b–7b

The salicylbenzothiazole ligands (**HL**¹–**HL**⁷) employed in this work are outlined in Scheme 1 and synthesized according to a published procedure.⁷⁵ The ligand structure was designed to have a similar structure to the analogous salicylbenzoxazole ligands used for the synthesis of aluminium complexes previously reported.⁷⁰ The substituents at the phenoxy rings include different combinations of electron withdrawing groups of different bulkiness (Cl and Br) and the ones with different steric demands (H, Me, ^tBu, Ph, and CMePh₂). Ligands **HL**¹–**HL**³ were obtained in moderate to good yields (51–77%) *via* condensation reactions of the corresponding salicylaldehyde with *o*-aminothiophenol, followed by oxidative cyclization in ethanol at 80 °C for 8 h. In the cases of ligands **HL**⁴–**HL**⁷ with bulky phenoxy substituents, the addition of ZrOCl₂·8H₂O as an oxidant was required for the intramolecular cyclization of 2-((2-mercaptophenylimino)methyl)phenol derivatives.⁷⁶ These ligands were obtained as light yellow crystals after recrystallisation in ethanol at –20 °C (45–80%).

The reaction of the ligand precursors **HL**¹–**HL**⁷ with one molar equivalent of trimethylaluminium (TMA) in toluene at room temperature afforded the four-coordinate aluminium complexes **1a–7a** in good yields (66–94%) as shown in Scheme 2. The five-coordinate aluminium complexes **1b–7b** were obtained by the reaction between TMA and the corresponding ligands in the 1:2 molar ratio in toluene at 100 °C in moderate to good yield (45–85%). ¹H NMR and ¹³C NMR experiments indicated well-resolved resonances for all proton and carbon environments. The purity of the compounds was verified by elemental analysis.



Scheme 1. The synthetic route for proligands **HL**¹–**HL**⁷.



Scheme 2. Synthetic routes for four-coordinate aluminium complexes (**1a–7a**) and five-coordinate aluminium complexes (**1b–7b**) from **HL**¹–**HL**⁷.

The ^1H NMR spectra of complexes **1a–7a** and **1b–7b** in CDCl_3 solution at 298 K contain a single set of resonances, indicative of the existence of a highly symmetric species on the NMR time scale (see Fig. S1–S14 in ESI). The symmetrical behavior detected by solution NMR experiments was also observed for the analogous aluminium salicylbenzoxazole complexes previously reported.⁷⁰ The formation of aluminium complexes was confirmed by the disappearance of the O–H proton signals of the free ligands and the appearance of the new Al–CH₃ proton signals as a singlet in the high field region (–0.90 to –0.52 ppm).^{77–79} The observation of one sharp singlet of two magnetically equivalent aluminium methyl groups of the four-coordinate aluminium complexes **1a–7a** could be attributed to the symmetric environment around the aluminium center. In the cases of the five-coordinate aluminium complexes **1b–7b**, the ^1H and ^{13}C NMR spectra reveal that both salicylbenzothiazole ligands exhibit magnetically equivalent environment upon coordination to the aluminium center.

Yellow crystals of complexes **5a** (Fig. 2) and **1b** (Fig. 3), suitable for single-crystal X-ray diffraction, were grown from a mixed solution of CH_2Cl_2 /hexane at 4 °C and from a saturated toluene solution at room temperature, respectively. The crystal of complex **5a** contains two crystallographically independent molecules as shown in Fig. 2 and Fig. S15 in ESI. Fig. 3 shows the X-ray structure of complex **1b**, which contains two independent complex molecules having fundamentally the same conformation and one toluene molecule (see Fig. S15–S18 and Tables S1–S6 in ESI for the crystallographic details).

Both independent complexes of **5a** feature a four-coordinate aluminium center in a distorted tetrahedral geometry (Fig. 2 and Fig. 15 in ESI) as seen in the bond angles for the first molecule: O(1)–Al(1)–C(22) [112.78(5)°], N(1)–Al(1)–C(22) [109.08(5)°], O(1)–Al(1)–C(23) [112.75(5)°] and O(1)–Al(1)–N(1) [93.48(4)°], and for the second molecule: O(2)–Al(2)–C(45) [116.39(5)°], N(2)–Al(2)–C(45) [105.34(5)°],

O(2)–Al(2)–C(46) [111.04(5)°] and O(2)–Al(2)–N(2) [93.28(4)°]. The extent of the distortion of tetrahedral geometry can be numerically determined by the geometry indices: $\tau = [360 - (\alpha + \beta)]/[360 - 2\theta]$ ⁸⁰ and $\tau' = [(\beta - \alpha)/(360 - \theta)] + [(180 - \beta)/(180 - \theta)]$,⁸¹ where θ for both equations is 109.5°. The average τ and τ' values are 0.91 and 0.90, indicative of the distorted tetrahedral geometry of the aluminium centers. The aluminium center coordinated with the phenolate oxygen and the benzothiazole nitrogen forms a six-membered N,O-chelated ring structure. The significant decrease in bond angles involving two coordinated atoms, the phenolate oxygen and the benzothiazole nitrogen, (O(1)–Al(1)–N(1) [93.48(4)°] and O(2)–Al(2)–N(2) [93.28(4)°]) from the ideal tetrahedral angle enhances the rigidity of the ligand backbone. Furthermore, all atoms regarding the six-membered chelated ring, except aluminium, are nearly in co-planarity as the atoms lie less than 0.11 Å away from the planes averaged from the O–C–C–N atoms. The dihedral angles between benzothiazole ring and phenoxy rings of the two independent molecules are equal to 16.90° (N(1)–C(7)–C(6)–C(1)) and 14.83° (N(2)–C(30)–C(29)–C(24)). The Al–C bond lengths (Al(1)–C(22) [1.9615(12) Å], Al(1)–C(23) [1.9555(12) Å], Al(2)–C(45) [1.9649(12) Å], and Al(2)–C(46) [1.9604(12) Å] conform with the values reported in the literature.^{48,49,82–84} The Al–N distances, Al(1)–N(1) [1.9717(10) Å] and Al(2)–N(2) [1.9636(10) Å] display the coordinative covalent bond character,^{82–87} while the Al–O bond lengths, Al(1)–O(1) [1.7712(8) Å] and Al(2)–O(2) [1.7743(8) Å] reveal the characteristic of σ -bonding.^{82–87}

Both the independent complexes of **1b** were monomeric with a five-coordinate aluminium center in a geometry best described as distorted trigonal bipyramidal (Fig. 3 and Fig. S17 in ESI). The amount of distortion can be calculated using the geometric criterion $\tau = (\beta - \alpha)/60$.^{88,89} The averaged τ value of **1b** is 0.77 which is slightly higher than that of the corresponding five-coordinate aluminium complexes bearing salicylbenzoxazole ligands previously reported ($\tau = 0.75$).⁷⁰ Regarding coordination geometries around the Al centers,

the two nitrogen atoms from different molecules of the ligand are located at the axial positions of the trigonal bipyramidal geometry. The diaxial angles, N(1)–Al(1)–N(2) [167.99(5)°] and N(3)–Al(2)–N(4) [168.13(5)°], are slightly distorted from linear resulting in the distorted trigonal bipyramidal shape. The equatorial planes consist of two oxygen atoms from different ligand molecules and one carbon of the methyl group. The equatorial angles at the aluminium center fall within the narrow range from 118.47(6)° for O(2)–Al(1)–C(27) to 122.35(6)° for O(1)–Al(1)–C(27). The Al–N bond lengths of 2.1125(12) Å [Al(1)–N(1)], 2.0964(13) Å [Al(1)–N(2)], 2.0933(13) Å [Al(2)–N(3)] and 2.0870 (13) Å [Al(2)–N(4)] are characteristic of the coordinative covalent bond,⁸²⁻⁸⁷ while the Al–O bond distances for Al(1)–O(1) [1.7716(12) Å], Al(1)–O(2) [1.7757(12) Å], Al(2)–O(3) [1.7729(11) Å] and Al(2)–O(4) [1.7723(11) Å] are more akin to σ -bond character.⁸²⁻⁸⁷ The Al–C bond lengths in **1b** [1.9656(17) Å and 1.9743(16) Å] are typical.^{48,49,82-87}

View Article Online
DOI: 10.1039/C7DT02435E

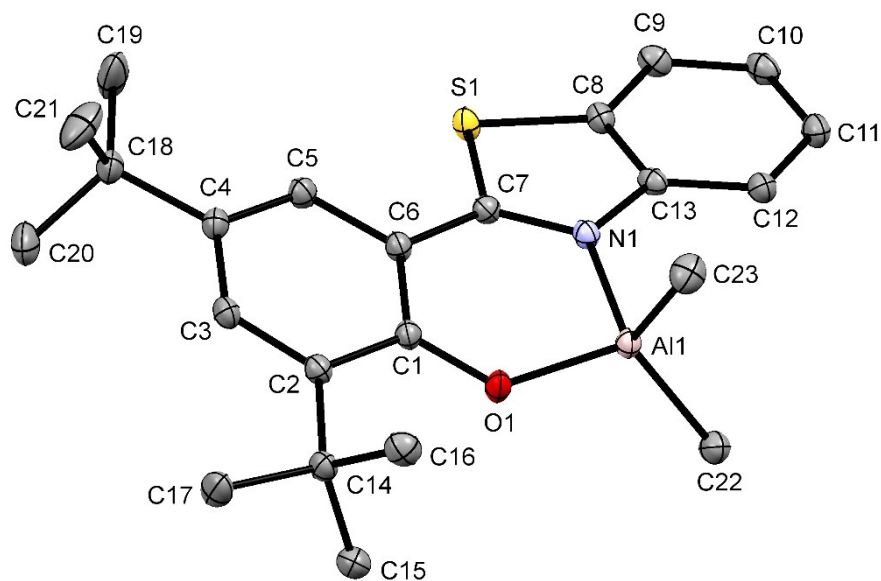


Fig. 2 ORTEP representation of **5a** with the thermal ellipsoids drawn at 50% probability level.

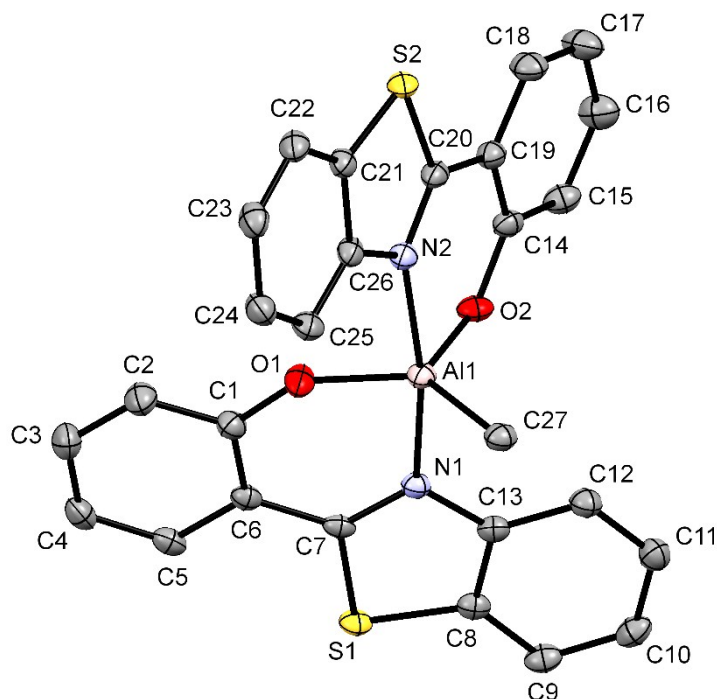


Fig. 3 ORTEP representation of **1b** with the thermal ellipsoids drawn at 50% probability level.

Ring-opening polymerisation of *rac*-lactide

View Article Online
DOI: 10.1039/C7DT02435E

The new aluminium salicylbenzothiazole complexes **1a–7a** and **1b–7b** were tested as initiators for the ROP of *rac*-LA in the presence of one equivalent of benzyl alcohol and the results are collected in Table 1. The polymerisations were carried out in toluene at 70 °C and the molar ratio of *rac*-LA to initiator was fixed at 100:1 ($[LA]_0/[Al] = 100$; $[LA]_0 = 0.83$ M; $[Al] = 8.33$ mM; M_n (theory) = 14400). The polymerisation progress was monitored by taking regular aliquots which were subsequently analyzed by 1H NMR spectroscopy to determine the conversion. The molecular weights and molecular weight distributions (M_w/M_n) were determined by gel permeation chromatography (GPC) using the Mark-Houwink correction of 0.58.⁹⁰⁻⁹² The experimental molecular weights of all the polymers produced with the aluminium complexes employed in this study were closed to the theoretical values calculated for a single PLA chain produced per metal center and the resulting polymers had unimodal and narrow molecular weight distributions ($M_w/M_n = 1.03–1.22$), indicative of full activation of the catalyst and controlled living polymerisations. The results also suggested only one methyl group of four-coordinate aluminium complexes **1a–7a** was converted to the benzyloxy initiating group. The polymerisations employing the four-coordinate aluminium complexes **1a–4a** and **6a** proceeded to more than 90% conversion in 24 h whereas that using complex **5a** reached 86% conversion in 24 h. The lowest activity in this series was observed for complex **7a** (96% conversion in 96 h). Similar to the previously reported aluminium salicylbenzoxazole complexes,⁷⁰ the polymerisation employing five-coordinate aluminium salicylbenzothiazole complexes was slower than that of four-coordinate aluminium counterparts. For example, complexes **1b–3b** polymerized *rac*-LA to *ca.* 90% conversion in 192 h and the least active initiator was complex **6b** which provided 86% conversion in 480 h.

Table 1. Polymerisation of *rac*-LA Using Complexes **1a–7a** and **1b–7b** in the Presence ofBenzyl Alcohol^a

entry	complex	time (h)	conv ^b (%)	M_n (theory) ^c (g mol ⁻¹)	M_n (GPC) ^d (g mol ⁻¹)	M_w/M_n ^d	P_m ^e	k_{app} ^f (10 ⁵ s ⁻¹)
1	1a	24	96	14 000	14 200	1.19	0.52	4.0 ± 0.1
2	1b	192	93	13 500	13 700	1.17	0.61	0.54 ± 0.1
3	2a	24	95	13 800	12 200	1.12	0.52	3.5 ± 0.1
4	2b	192	90	13 100	12 900	1.22	0.57	0.37 ± 0.1
5	3a	24	93	13 500	11 200	1.12	0.45	3.2 ± 0.1
6	3b	192	91	13 200	12 300	1.15	0.62	0.35 ± 0.01
7	4a	24	93	13 500	13 100	1.15	0.44	2.5 ± 0.1
8	4b	192	80	11 600	11 200	1.08	0.60	0.30 ± 0.01
9	5a	24	86	12 500	11 400	1.09	0.62	1.9 ± 0.1
10	5b	48	91	13 200	12 700	1.09	0.61	1.3 ± 0.1
11	6a	24	94	13 600	13 600	1.19	0.52	2.9 ± 0.1
12	6b	480	86	12 500	9 600	1.08	0.57	0.13 ± 0.1
13	7a	96	96	13 900	13 200	1.19	0.66	1.2 ± 0.1
14	7b	192	92	13 400	12 500	1.03	0.60	0.22 ± 0.2

^a[LA]₀/[Al] = 100, [Al]/[PhCH₂OH] = 1, [LA]₀ = 0.83 M, [Al] = 8.33 mM, toluene, 70 °C. ^bAs determined *via* integration of the methine resonances (¹H NMR) of LA and PLA (CDCl₃, 400 MHz). ^cCalculated by $[(\text{[LA]}_0/\text{[Al]}) \times 144.13 \times \text{conversion}] + 108.14$. ^dDetermined by gel permeation chromatography (GPC) calibrated with polystyrene standards in THF and corrected by a factor of 0.58 for PLA. ^e P_m is the probability of *meso* linkage between monomer units and was calculated from the homonuclear decoupled ¹H NMR spectrum of the obtained poly(*rac*-LA): $[mmm] = P_m^2 + (1 - P_m)P_m/2$; $[mmr] = [rmm] = (1 - P_m)P_m/2$; $[rmr] = (1 - P_m)^2/2$; $[mrm] = [(1 - P_m)^2 + (1 - P_m)P_m]/2$. ^f[LA]₀/[Al] = 50, [Al]/[PhCH₂OH] = 1, [LA]₀ = 0.42 M, [Al] = 8.33 mM, toluene, 70 °C.

The well-controlled living polymerisation and a single-site reaction for this catalyst system were also highlighted by the observation of a linear correlation between M_n and the percent conversion (Fig. 4 and Fig. S19–S31 in ESI). Furthermore, the relatively narrow observed PDI values (<1.2) throughout the course of polymerisation suggested that the polymerisation proceeded without a significant degree of transesterifications.^{34,60}

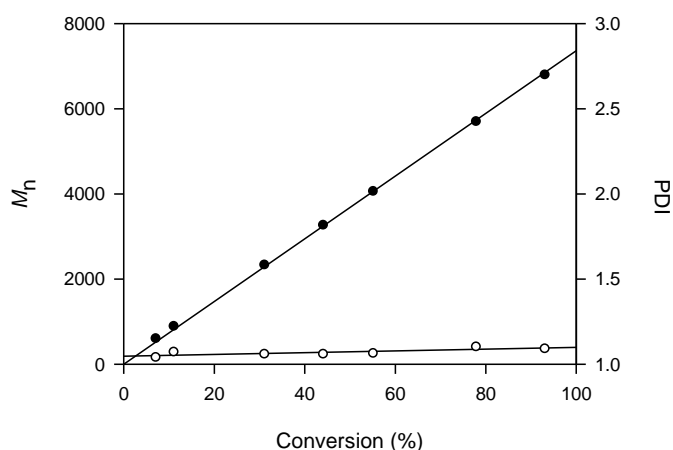


Fig. 4 Plot of PLA M_n (●) (versus polystyrene standards) and PDI (○) as a function of monomer conversion for a *rac*-LA polymerisation using **3a**/PhCH₂OH ([LA]₀/[Al] = 50, toluene, 70 °C).

Four-coordinate aluminium complexes **1a–7a** were also evaluated for *rac*-LA polymerisation activity in the presence of excess benzyl alcohol to investigate their catalytic performance for the immortal ROP of *rac*-LA.⁹³⁻¹⁰¹ The ratio of benzyl alcohol was increased from 2 to 10 on a constant [LA]₀/[Al] ratio of 100. Excess benzyl alcohol molecules act as chain-transfer agents (CTAs) which involve in a rapid and reversible exchange with the growing alkoxide chain. As shown in Table 2, in all cases, the molecular weights of the resulting polymers decreased with increasing amount of benzyl alcohol and the observed molecular weights were in good agreement with the theoretical values that were proportional to the initial [LA]₀/[PhCH₂OH] ratio. The PDI values were also relatively narrow even at a high amount of benzyl alcohol added. These observations suggested that a fast, reversible exchange between dormant hydroxyl-end-capped polymer chains/free benzyl alcohol and the active growing alkoxide chain coordinated onto the aluminium center occurred significantly

faster than the chain propagation.^{70,96} Thus, the results were consistent with controlled alcohol-mediated chain transfer reactions during the ring-opening polymerisation.

Table 2. Polymerisation of *rac*-LA using Complexes **1a–7a** in the Presence of Benzyl Alcohol^a

entry	complex	[LA] ₀ : [Al]: [PhCH ₂ OH]	time (h)	conv ^b (%)	<i>M_n</i> (theory) ^c (g mol ⁻¹)	<i>M_n</i> (GPC) ^d (g mol ⁻¹)	<i>M_w</i> / <i>M_n</i> ^d
1	1a	100:1:2	9	93	6 800	6 500	1.20
2	2a	100:1:2	9	81	5 900	5 400	1.12
3	3a	100:1:2	9	88	6 400	5 900	1.14
4	4a	100:1:2	9	87	6400	5 800	1.10
5	5a	100:1:2	24	94	6 900	7 200	1.09
6	6a	100:1:2	9	73	5 400	4 600	1.09
7	7a	100:1:2	24	64	4 700	4 000	1.05
8	1a	100:1:5	6	88	2 600	2 000	1.19
9	2a	100:1:5	6	81	2 400	2 000	1.09
10	3a	100:1:5	6	93	2 800	2 800	1.11
11	4a	100:1:5	6	90	2 700	2 200	1.12
12	5a	100:1:5	9	87	2 600	2 400	1.10
13	6a	100:1:5	6	70	2 100	1 600	1.12
14	7a	100:1:5	24	74	2 200	2 000	1.07
15	1a	100:1:10	6	89	1 400	1 100	1.17
16	2a	100:1:10	6	87	1 400	1 000	1.10
17	3a	100:1:10	6	88	1 400	1 100	1.17
18	4a	100:1:10	6	85	1 300	1 100	1.14
19	5a	100:1:10	6	85	1 300	1 000	1.14
20	6a	100:1:10	6	82	1 300	1 000	1.15
21	7a	100:1:10	24	77	1 200	1 000	1.11

^a[LA]₀/[Al] = 100, [LA]₀ = 0.83 M, [Al] = 8.33 mM, toluene, 70 °C. ^bAs determined *via* integration of the methine resonances (¹H NMR) of LA and PLA (CDCl₃, 500 MHz). ^cCalculated by (([LA]₀/[Al]) × 144.13 × conversion)/[PhCH₂OH] + 108.14. ^dDetermined by gel permeation chromatography (GPC) calibrated with polystyrene standards in THF and corrected by a factor of 0.58 for PLA.

Kinetic studies of *rac*-LA polymerisation

View Article Online
DOI: 10.1039/C7DT02435E

To study the reaction kinetics of the ROP process of *rac*-LA initiated by complexes **1a–7a** and **1b–7b**, all polymerisations were carried out in toluene at 70 °C in the presence of one equivalent of benzyl alcohol ($[LA]_0/[Al] = 50$; $[Al] = 8.33$ mM; $[LA]_0 = 0.42$ M). The progress of polymerisations was monitored by taking regular aliquots of the polymerisation solution, which were then analyzed by 1H NMR spectroscopy. Fig. 5 shows the semilogarithmic plot of the *rac*-LA conversion ($\ln([LA]_0/[LA]_t)$) versus time for the polymerisations using **1a** and **1b** (see also Fig. S32–S37 in ESI for the plots of other complexes). In all cases, the linear relationship was illustrated, indicating the apparent first-order kinetics in the monomer. Furthermore, a straight line passing through the origin of the plot designated that the active aluminium alkoxide species was formed instantaneously by an *in situ* alcoholysis reaction utilizing benzyl alcohol. Hence, the polymerisation proceeded according to the rate law $-d[LA]/dt = k_{app}[LA]$, where $k_{app} = k_p[Al]^x$, in which k_p is the propagation rate constant.

To determine the order in aluminium (x), kinetic experiments were conducted with variable concentrations of the catalyst from 8.33 to 24.96 mM under identical conditions ($[LA]_0 = 0.42$ M). Accordingly, Fig. 6 shows the semilogarithmic plots of *rac*-LA conversions versus time using five different concentrations of complex **1a**. The order in aluminium was obtained from the gradient (x) of the plot of $\ln k_{app}$ versus $\ln [Al]$, as shown in Fig. 7. The obtained x value of 0.98 (*ca.* 1.0) signified the first-order kinetics in aluminium concentration. The k_p value of $4.27 \times 10^{-3} \text{ s}^{-1} \text{ mol}^{-1} \text{ L}$ was obtained from the gradient of the plot between k_{app} versus $[Al]$, as shown in Fig. 8. Therefore, the overall rate equation is $-d[LA]/dt = k_p[LA][\mathbf{1a}]$. The stoichiometric involvement of two species, *i.e.* the active aluminium benzyloxide and lactide, in the overall rate law indicated that the ROP of *rac*-LA follows a monometallic coordination-insertion mechanism with the coordination of monomer

to the aluminium center, followed by the ring-opening process.⁷⁰ The order of aluminium for the ROP of *rac*-LA mediated by complex **1b** was also determined using the same procedure (see also Fig. S38–S40 in ESI). The order x of 0.99 (*ca.* 1.0) and the k_p value of $3.53 \times 10^{-4} \text{ s}^{-1} \text{ mol}^{-1} \text{ L}$ were obtained, establishing the overall rate law in the form of $-\text{d}[\text{LA}]/\text{dt} = k_p[\text{LA}][\mathbf{1b}]$.

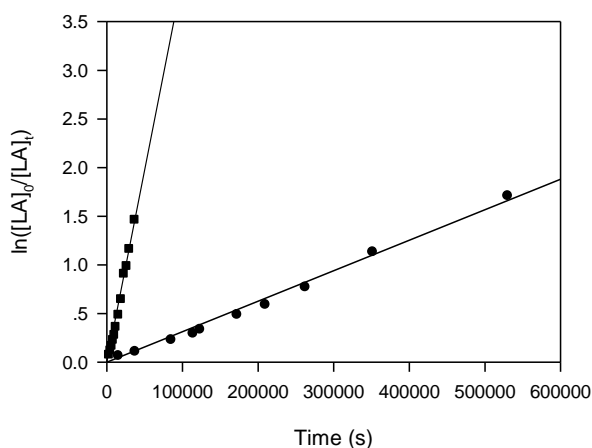


Fig. 5 Semilogarithmic plots of *rac*-lactide conversion versus time in toluene at 70 °C with complexes **1a** (■) and **1b** (●) ($[\text{LA}]_0/[\text{Al}] = 50$, $[\text{Al}]/[\text{PhCH}_2\text{OH}] = 1$, $[\text{LA}]_0 = 0.42 \text{ M}$, $[\text{Al}] = 8.33 \text{ mM}$).

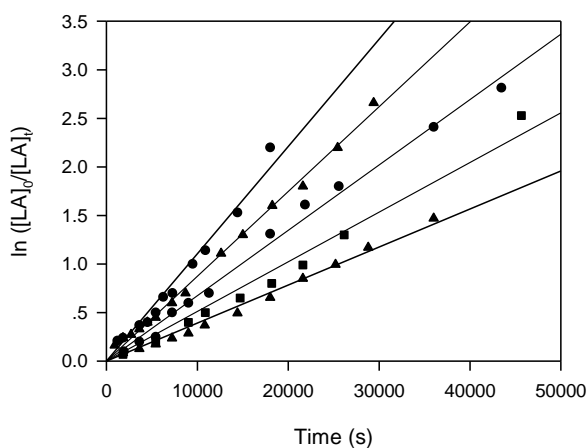


Fig. 6 Semilogarithmic plots of the *rac*-lactide conversion versus time in toluene at 70 °C with complex **1a**/ PhCH_2OH as an initiator ($[\text{LA}]_0 = 0.42 \text{ M}$: **I**, $[\text{Al}] = 24.99 \text{ mM}$, $[\text{LA}]_0/[\text{Al}] = 17$; **II**, $[\text{Al}] = 20.82 \text{ mM}$, $[\text{LA}]_0/[\text{Al}] = 20$; **III**, $[\text{Al}] = 16.67 \text{ mM}$, $[\text{LA}]_0/[\text{Al}] = 25$; **IV**, $[\text{Al}] = 12.50 \text{ mM}$, $[\text{LA}]_0/[\text{Al}] = 34$; **V**, $[\text{Al}] = 8.33 \text{ mM}$, $[\text{LA}]_0/[\text{Al}] = 50$).

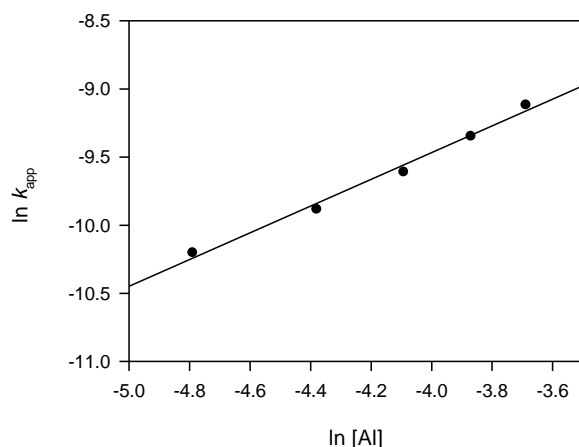


Fig. 7 Plot of $\ln k_{\text{app}}$ versus $\ln [\text{Al}]$ for the polymerisation of *rac*-lactide with complex **1a**/PhCH₂OH as an initiator (toluene, 70 °C, [LA]₀ = 0.42 M).

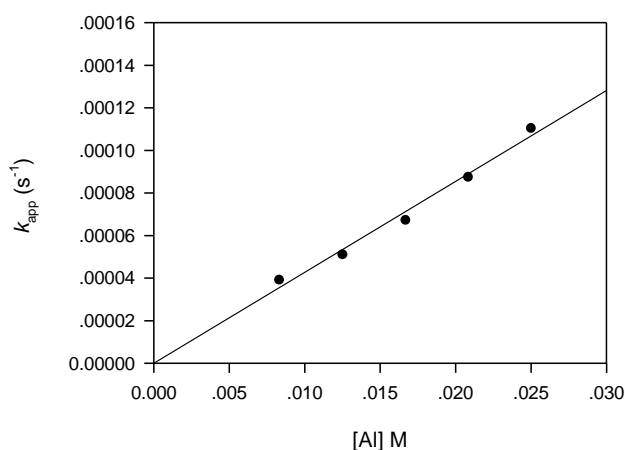


Fig. 8 Plot of k_{app} versus $[\text{Al}]$ for the polymerisation of *rac*-lactide with complex **1a**/PhCH₂OH as an initiator (toluene, 70 °C, [LA]₀ = 0.42 M).

According to the apparent rate constant values (k_{app}) summarized in Table 1, each four-coordinate aluminium complex was more active toward *rac*-LA polymerisation than its five-coordinate congener. For example, the k_{app} value of four-coordinate aluminium complex **1a** ($(4.0 \pm 0.1) \times 10^{-5} \text{ s}^{-1}$) was *ca.* 7 times higher than that of five-coordinate aluminium complex **1b** ($(0.54 \pm 0.1) \times 10^{-5} \text{ s}^{-1}$). The decrease in polymerisation activity was attributed to the increase of steric shielding of the aluminium center by the presence of two ancillary

ligands. The data also demonstrated that the size of the alkyl phenoxy substituents had a notable influence on the catalytic behavior of the complexes. For the four-coordinate aluminium complexes **1a–7a**, the catalytic activity decreased in the order *o,p*-H (**1a**) > *o,p*-Me (**2a**) > *o,p*-^tBu (**5a**) when the size of the alkyl phenoxy substituents at the *ortho*- and *para*-positions increased from H to Me to ^tBu. According to our previous work, the steric factor from the *para*-substituent of the closely related salicylbenzoxazole ligands has no substantial impact on the catalytic performance of the complexes.⁷⁰ Therefore, in the cases of complexes **6a** and **7a** containing the bulky group at the *ortho* position of the phenoxy ring, the catalytic activity reduced as the size increased from **6a** (*o*-Ph, *p*-H) > **7a** (*o*-CMePh₂, *p*-Me). The observed lower activity was attributed to the steric protection at the aluminium center by the bulky substituent, which hindered the incorporation of the monomer into the growing polymer chain.^{102,103} In comparison with complex **2a** (*o,p*-Me), the introduction of the electron withdrawing Cl atoms at the *ortho*- and *para*-positions of the phenoxy unit (**3a**) resulted in a diminished catalytic activity, which can be ascribed to the different sensitivities between the coordination and insertion steps to the Lewis acidity of the metal center. The enhanced Lewis acidity induced by electron-withdrawing substituents may lead to preferred coordination and activation, but it may also hinder the subsequent insertion step as a result of a stronger binding of the growing alkoxide chain to the metal center.¹⁰⁴⁻¹⁰⁷ Furthermore, the lower activity of complexes **3a** may also be attributed to the electron-donating conjugated effect from the lone pair electron on the Cl atom, leading to the unfavorable coordination of the lactide monomer.⁵⁵ A decrease in catalytic activity when incorporating the halogen substituent at the ancillary ligands was also observed in other catalytic systems.^{55,108} Replacing the chlorine atoms with the less electronegative bromine atoms (**4a**) resulted in the reduction of the catalytic activity. Therefore, the catalytic activity of the four-coordinate

View Article Online
DOI: 10.1039/C7DT02435E

Dalton Transactions Accepted Manuscript

aluminium complexes decreased in the order of **1a** (*o,p*-H) > **2a** (*o,p*-Me) > **3a** (*o,p*-Cl) > **6a** (*o*-Ph, *p*-H) > **4a** (*o,p*-Br) > **5a** (*o,p*-^tBu) > **7a** (*o*-CMePh₂, *p*-Me).

For the five-coordinate aluminium complexes **1b-7b**, the steric factor of the alkyl phenoxy substituent affected the catalytic activity in the order of **5b** (*o,p*-^tBu) > **1b** (*o,p*-H) > **2b** (*o,p*-Me) > **7b** (*o*-CMePh₂, *p*-Me) > **6b** (*o*-Ph, *p*-H). In contrast to the four-coordinate aluminium complexes, the five-coordinate aluminium complex **5b** bearing ^tBu phenoxy substituents exhibited the highest k_{app} value of $(1.3 \pm 0.1) \times 10^{-5} \text{ s}^{-1}$ whereas complex **6b** featuring the *ortho*-phenyl substituents at the phenoxy ring displayed the lowest k_{app} value of $(0.13 \pm 0.01) \times 10^{-5} \text{ s}^{-1}$. In addition, the halogen substituents **3b** (*o,p*-Cl) and **4b** (*o,p*-Br) did not show significant influence on the catalytic activity, *i.e.* the k_{app} values of **3b** and **4b** were comparable and also similar to those of **2b** (*o,p*-Me) ($k_{app} = (0.37 \pm 0.1) \times 10^{-5} \text{ s}^{-1}$ for **2b**; $k_{app} = (0.35 \pm 0.01) \times 10^{-5} \text{ s}^{-1}$ for **3b**; $k_{app} = (0.30 \pm 0.01) \times 10^{-5} \text{ s}^{-1}$ for **4b**). In the series of five-coordinate complexes, the rates of polymerisation decreased in the order **5b** (*o,p*-^tBu) > **1b** (*o,p*-H) > **2b** (*o,p*-Me) \approx **3b** (*o,p*-Cl) \approx **4b** (*o,p*-Br) > **7b** (*o*-CMePh₂, *p*-Me) > **6b** (*o*-Ph, *p*-H).

The kinetic data revealed that the steric and electronic influences were more pronounced in the series of four-coordinate aluminium complexes than their homologous five-coordinate aluminium complexes. Moreover, it was found that the aluminium salicylbenzothiazole complexes were less active than their aluminium salicylbenzoxazole analogs previously investigated.⁷⁰

Stereoselectivity of *rac*-LA polymerisation

The microstructure of the PLAs produced by complexes **1a-7a** and **1b-7b** was determined by analyzing the signal intensities of the methine region of the homonuclear decoupled ¹H NMR spectra.¹⁰⁹⁻¹¹⁴ All homonuclear decoupled ¹H NMR spectra are shown in Fig. S41-S54 in ESI. The microstructure of the obtained PLA samples was changed slightly

by the variation of the phenoxy substituents and the number of chelating ligands coordinated to the aluminium center. In the series of four-coordinate aluminium complexes **1a–7a**, complexes **1a**, **2a** and **6a** produced atactic PLAs with an identical P_m value of 0.52 whereas slight heterotactic-biased PLAs were prepared by complexes **3a** ($P_r = 0.55$) and **4a** ($P_r = 0.56$) containing chloro and bromo substituents at the phenoxy ring, respectively. In addition, isotactic-enriched PLAs were obtained when increasing the bulkiness of the *ortho* alkyl substituents installed on the phenoxy rings. For example, complex **5a** containing *tert*-butyl phenoxy substituents furnished isotactic PLA with the P_m value of 0.62. The most notable isotacticity was observed when exchanging the *ortho tert*-butyl substituent with CMePh₂ group, leading to an improvement of the P_m value to 0.66 for complex **7a**.

In the series of five-coordinate aluminium complexes, the introduction of the bulky phenoxy substituents did not bring further improvement of isoselectivity control. The P_m values of PLAs produced by complexes **1b**, **2b**, and **5b–7b** were in the range of 0.57–0.61. In marked contrast to four-coordinate aluminium complexes containing halogen substituents (**3a** and **4a**), five-coordinate aluminium complexes **3b** and **4b** gave rise to isotactic-biased PLAs ($P_m = 0.62$ and 0.60, respectively). It is noted that the P_m values of PLAs prepared by complexes **5a** and **5b** bearing *tert*-butyl phenoxy substituents were comparable ($P_m = 0.62$ for **5a** and $P_m = 0.61$ for **5b**), suggesting that the increased steric congestion at the aluminium center did not lead to an increase in the catalyst's ability to select the desired stereoisomer of the lactide. These observations were also exhibited in the related aluminium salicylbenzoxazole system in which the four-coordinate and five-coordinate aluminium complexes containing *tert*-butyl phenoxy substituents produced PLAs with the same level of isoselectivity control.⁷⁰ Furthermore, in the cases of complexes **7a** and **7b** bearing the bulky CMePh₂ at the *ortho* position of phenoxy unit, the degree of isoselectivity was diminished from $P_m = 0.66$ for **7a** to $P_m = 0.60$ for **7b**.

In comparison, the level of stereocontrol established in this aluminium salicylbenzothiazole system was found to be lower than that ascertained in the previously reported aluminium salicylbenzoxazole system. For the aluminium salicylbenzoxazole system, the isotactic-enriched PLA with the highest P_m value of 0.75 was prepared. However, in this system, the highest P_m value of 0.66 was achieved for PLA produced by complex **7a**.

To improve the degree of isoselectivity, the effect of polymerisation temperature was investigated by changing the polymerisation temperature from 70 °C to 50 °C. Employing complexes **5a** and **7a** for the *rac*-LA polymerisation ($[LA]_0/[Al]/[PhCH_2OH] = 100/1/1$, $[Al] = 8.33$ mM, toluene) gave rise to isotactic PLAs, yielding a higher P_m value of 0.66 and 0.70, respectively (**5a**: 96 h, 91%, $M_n = 13\ 900$, PDI = 1.16; **7a**: 192 h, 87%, $M_n = 11\ 200$, PDI = 1.07) (see Fig. S55 and S56 in ESI). Therefore, the degree of isoselectivity was increased with the decrease of polymerisation temperature.

End-group analysis by 1H NMR spectroscopy and MALDI-TOF spectrometry

To gain more information on the mechanism entailed in the polymerisation of *rac*-LA, an end group analysis was carried out by 1H NMR spectroscopy in $CDCl_3$ at 298 K. The low molecular weight polylactide was prepared by conducting a polymerisation experiment at a low $[LA]_0/[Al]$ ratio of 40. As shown in Fig. 9, 1H NMR analysis of this PLA sample disclosed a hydroxyl end group ($H_c = -CH(CH_3)OH$) and a benzyl ester end group ($H_e = -COOCH_2C_6H_5$) with the integration ratio of $H_c:H_e = 1:5$. These results indicated that the terminal alkoxide $-OCH_2Ph$ moiety is the only initiating group involved in the polymerisation process. Therefore, a coordination-insertion mechanism, involving selective cleavage of the acyl-oxygen bond of the lactide monomer and the insertion into the alkoxide-aluminium bond, should be operative in this system.^{115,116}

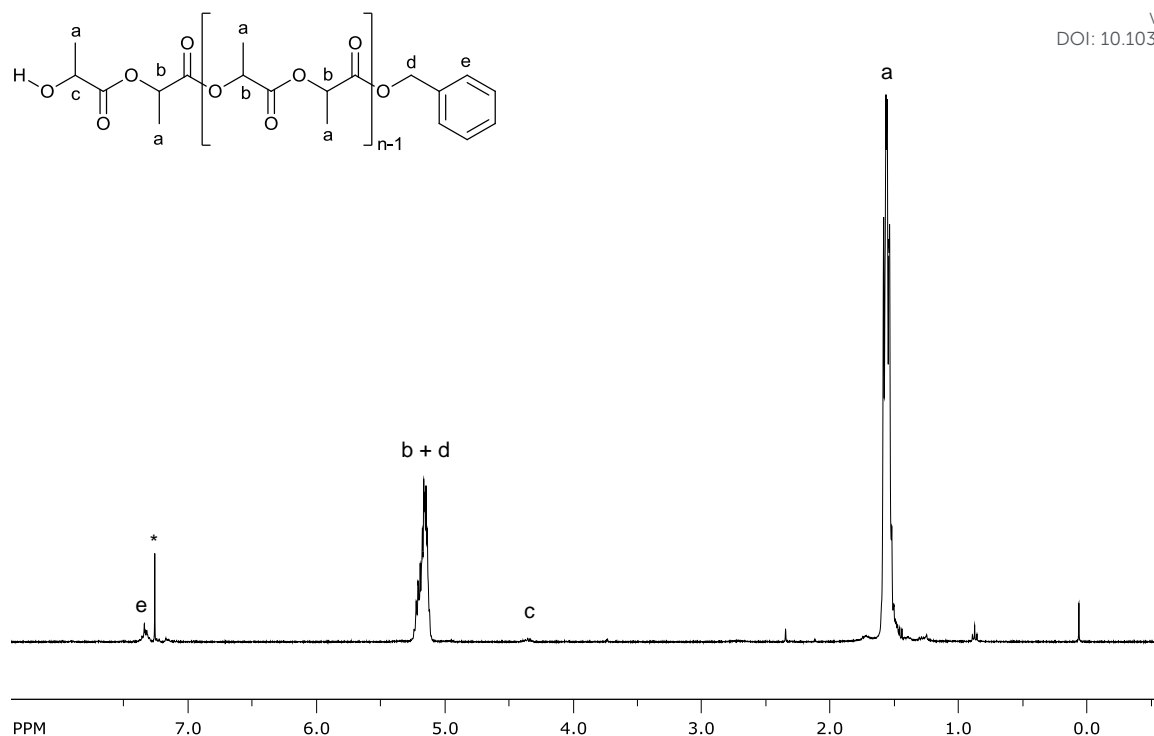


Fig. 9 ^1H NMR spectrum of the low molecular weight PLA initiated by **1a**/ PhCH₂OH in CDCl₃ at 298 K (* = solvent residue peak).

The formation of linear polylactide capped with a benzyloxy group at one end and a hydroxyl group at the other end was also investigated by MALDI-TOF mass spectrometry. Fig. 10 shows the mass spectrum of polylactide prepared by **7b**/ PhCH₂OH (Table 1, entry 14). The spectrum shows two sets of peak distributions and each set displays a $\Delta(m/z)$ separation of 144 Da, corresponding to the repeating unit of *rac*-LA. The set of high intensity peaks is assigned to polylactide chains end-capped with the benzyloxy groups ($-\text{OCH}_2\text{Ph}$) clustered with sodium ions to give adducts $\text{PhCH}_2\text{O}-[\text{C}(\text{O})\text{CH}(\text{CH}_3)\text{OC}(\text{O})\text{CH}(\text{CH}_3)\text{O}]_m-\text{H} + \text{Na}$ (e.g. $n = 80$, $m/z = 11663.297$) whereas the set of lower intensity peaks correspond to the polymers of the form $\text{PhCH}_2\text{OC}(\text{O})\text{CH}(\text{CH}_3)\text{O}-[\text{C}(\text{O})\text{CH}(\text{CH}_3)\text{OC}(\text{O})\text{CH}(\text{CH}_3)\text{O}]_n-\text{H} + \text{Na}$ (e.g. $n = 80$, $m/z = 11735.507$). The results obtained from the MALDI-TOF MS are in good agreement with ^1H NMR spectroscopic analysis, supporting the ring-opening polymerisation occurs via a coordination-insertion mechanism. In addition, there are no peak

envelopes with a $\Delta(m/z)$ difference of 72 Da, which is a half unit of lactide ($-\text{OCH}(\text{CH}_3)\text{C}(\text{O})-$), appeared in the mass spectrum. Hence, there is no evidence for transesterification side reactions during the polymerisation.

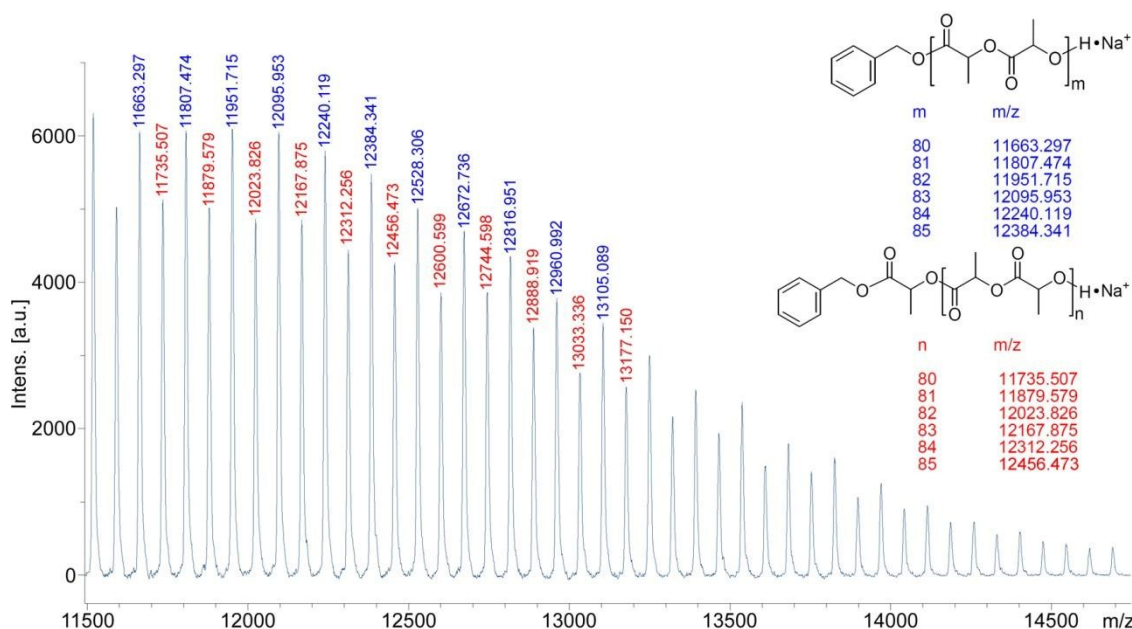


Fig. 10 MALDI-TOF mass spectrum of PLA initiated by **7b**/PhCH₂OH in toluene at 70°C, [LA]₀/[Al] = 100, [Al]/[PhCH₂OH] = 1, [LA]₀ = 0.83 M, [Al] = 8.33 mM (Table 1, entry 14).

Ring-opening polymerisation of ϵ -caprolactone

The ring-opening polymerisations of ϵ -caprolactone (ϵ -CL) using complexes **1a–7a** and **1b–7b** were also explored to assess the control of the polymerisation under the same conditions for those of *rac*-LA. The results are shown in Table 3. All complexes polymerized ϵ -CL in controlled manner as evidenced by the experimental molecular weights closed to the theoretical values and the narrow PDIs in the range of 1.24–1.55. As for polymerisations of *rac*-LA, the four-coordinate aluminium complexes (**1a–7a**) were more active than their five-coordinate aluminium counterparts (**1b–7b**). All polymerisations employing complexes

1a–7a proceeded to more than 99% within 15 min. In the series of five-coordinate aluminium complexes, complexes **3b**, **4b** and **5b** were more active toward the ROP of ϵ -CL and reached completion within 15 min. It was also apparent that the polymerisation activity was enhanced as the size of alkyl phenoxy substituents increased. For example, the catalytic activity decreased in the order *o*-CMePh₂, *p*-Me (**7b**) > *o*-Ph, *p*-H (**6b**) > *o,p*-H (**1b**) \approx *o,p*-Me (**2b**). Similar trend was observed in the ROP of ϵ -CL using aluminium complexes bearing benzothiazole ligands.⁷⁴ In addition, the catalytic activity of aluminium salicylbenzothiazole complexes could be classified as moderate to good performance according to the activity table for ϵ -CL polymerisation developed by Redshaw *et al.*⁶⁹

Table 3 Polymerisation of ϵ -caprolactone using **1a–7a** and **1b–7b** in the presence of benzyl alcohol.^a

entry	complex	time (min)	conv ^b (%)	M_n (theory) ^c (g mol ⁻¹)	M_n (GPC) ^d (g mol ⁻¹)	M_w/M_n ^d
1	1a	10	>99	11 500	11 700	1.35
2	1b	1080	>99	11 500	11 800	1.37
3	2a	15	>99	11 500	11 600	1.30
4	2b	1080	>99	11 500	11 300	1.45
5	3a	10	>99	11 500	8 900	1.55
6	3b	15	>99	11 500	11 600	1.38
7	4a	10	>99	11 500	11 800	1.27
8	4b	15	>99	11 500	11 800	1.41
9	5a	10	>99	11 500	9 900	1.46
10	5b	15	>99	11 500	11 200	1.44
11	6a	15	>99	11 500	12 400	1.30
12	6b	720	>99	11 500	11 500	1.36
13	7a	10	>99	11 500	12 000	1.44
14	7b	360	>99	11 500	13 400	1.24

^a $[\epsilon\text{-CL}]_0/[\text{Al}] = 100$, $[\text{Al}]/[\text{BnOH}] = 1$, $[\text{CL}]_0 = 1.67$ M, $[\text{Al}] = 16.7$ mM, toluene, 70 °C. ^bAs determined *via* integration of the methylene resonances (¹H NMR) of ϵ -CL and PCL (CDCl₃, 500 MHz). ^cCalculated by $[(\epsilon\text{-CL})_0/[\text{Al}]] \times 114.13 \times \text{conversion}] + 108.14$. ^dDetermined by gel permeation chromatography (GPC) calibrated with polystyrene standards in THF and corrected by a factor of 0.56 for PCL.

DFT Calculations

View Article Online
DOI: 10.1039/C7DT02435E

Density functional theory (DFT) calculations have been increasingly employed in the mechanistic study of ROP of various lactone monomers.^{24,32,36,45,106,117-127} To acquire further insight into the reaction mechanism and in particular to better understand the different catalytic activities observed in aluminium salicylbenzothiazole and aluminium salicylbenzoxazole systems, density functional theory (DFT) calculations were thus carried out. Aluminium salicylbenzothiazole complexes **1a** (four-coordinate complex) and **1b** (five-coordinate complex) and aluminium salicylbenzoxazole complexes **1a'** (four-coordinate complex) and **1b'** (five-coordinate complex) were selected as representatives. All calculations were carried out with the GAUSSIAN 09 program package¹²⁸ at the M06-2X level of theory¹²⁹⁻¹³¹ with the 6-311G(d,p) basis set.¹³² The validity of the methodology was verified by comparing the experimental geometrical parameters obtained from X-ray analysis of complexes **1b** and **1b'** with their optimized geometrical data. A good agreement regarding bond lengths and bond angles between the X-ray and the optimized structures was observed. Fig. 11 shows the optimized structure of complexes **1a**, **1a'**, **1b**, and **1b'** (see Tables S7 and S8 in ESI for their selected structural parameters).

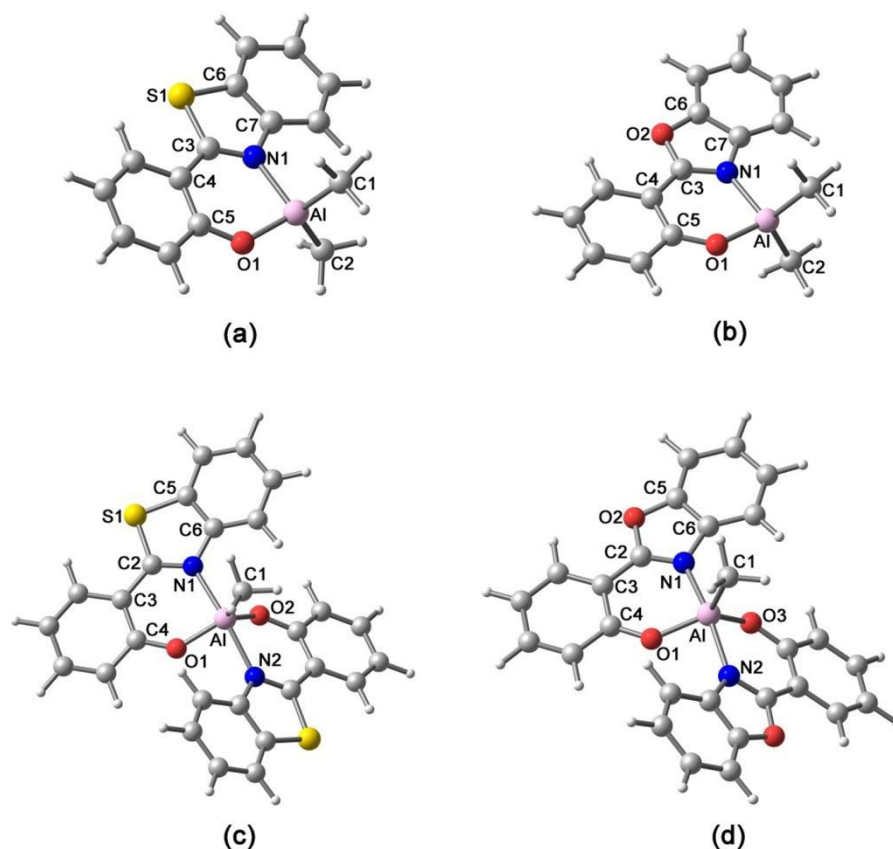


Fig. 11 Optimized structures of (a) **1a**, (b) **1a'**, (c) **1b** and (d) **1b'**.

Since the active species for the initiation of the ROP is a metal alkoxide complex, we started the reaction with the activated aluminium benzyloxy initiator. The Gibbs free energy profiles determined for the ROP of *L*-LA mediated by **1a**, **1a'**, **1b**, and **1b'** are presented in Fig. 12. The overall geometries of the transition states and key species proposed in the coordination-insertion mechanism are similar to those reported in literature (see Tables S9 and S10 in ESI for the structural parameters of key species).¹¹⁷⁻¹²⁷ The first step is the coordination of lactide to the aluminium center *via* the carbonyl oxygen of the lactide through the van der Waals complex (**R**). In the cases of four-coordinate aluminium initiators **1a** and **1a'**, the coordination adducts were formed as indicated by the distance between the carbonyl oxygen atoms of the lactide molecules and the aluminium center (Al–O_{carbonyl}) of 2.224 Å and 2.313 Å for **1a** and **1a'**, respectively, and the aluminium center is in a trigonal bipyramidal

coordination environment. However, for the five-coordinate aluminium initiators **1b** and **1b'**, the coordination adducts could not be located seemingly due to the steric congestion around the aluminium center. The geometries of aluminium initiators **1b** and **1b'** and lactide monomer in **R** compared with their initial geometries are very similar. The bond distances between aluminium center and the carbonyl oxygen O(4) of the lactide are equal to 3.223 Å for **1b** and 3.143 Å for **1b'**. Despite the elusive coordination adducts the benzyloxide and lactide were brought into proximity to accomplish alkoxide insertion step. The next step is the nucleophilic attack of the benzyloxide moiety to the carbonyl carbon of the coordinated lactide to form the tetrahedral intermediate (**INT1**). At the transition state (**TS1**), the C=O bond was slightly elongated as a result of a rehybridization of the carbonyl carbon from sp^2 to sp^3 . The formation of **INT2** by the rotation around the $O_{\text{alkoxide}}-C$ bond allowed the O_{acyl} to approach the aluminium center closely. Then, the polymerisation mechanism proceeded through the second transition state (**TS2**) which is the ring-opening step. At **TS2**, the dissociation of the LA $O_{\text{carbonyl}}-Al$ bond and the cleavage of the LA $O_{\text{acyl}}-C$ bond occurred concomitantly, along with the formation of new alkoxide bond. Further reorganization of the growing polymer chain resulted in the formation of a five-membered metallocyclic product (**P**). Overall, the free energy for the insertion of the first monomer unit is exergonic in all cases (see Fig. S57–S60 in ESI for the schematic illustration of the optimized geometries during the ring-opening step of L-LA mediated by the initiators **1a**, **1a'**, **1b**, and **1b'**, respectively).

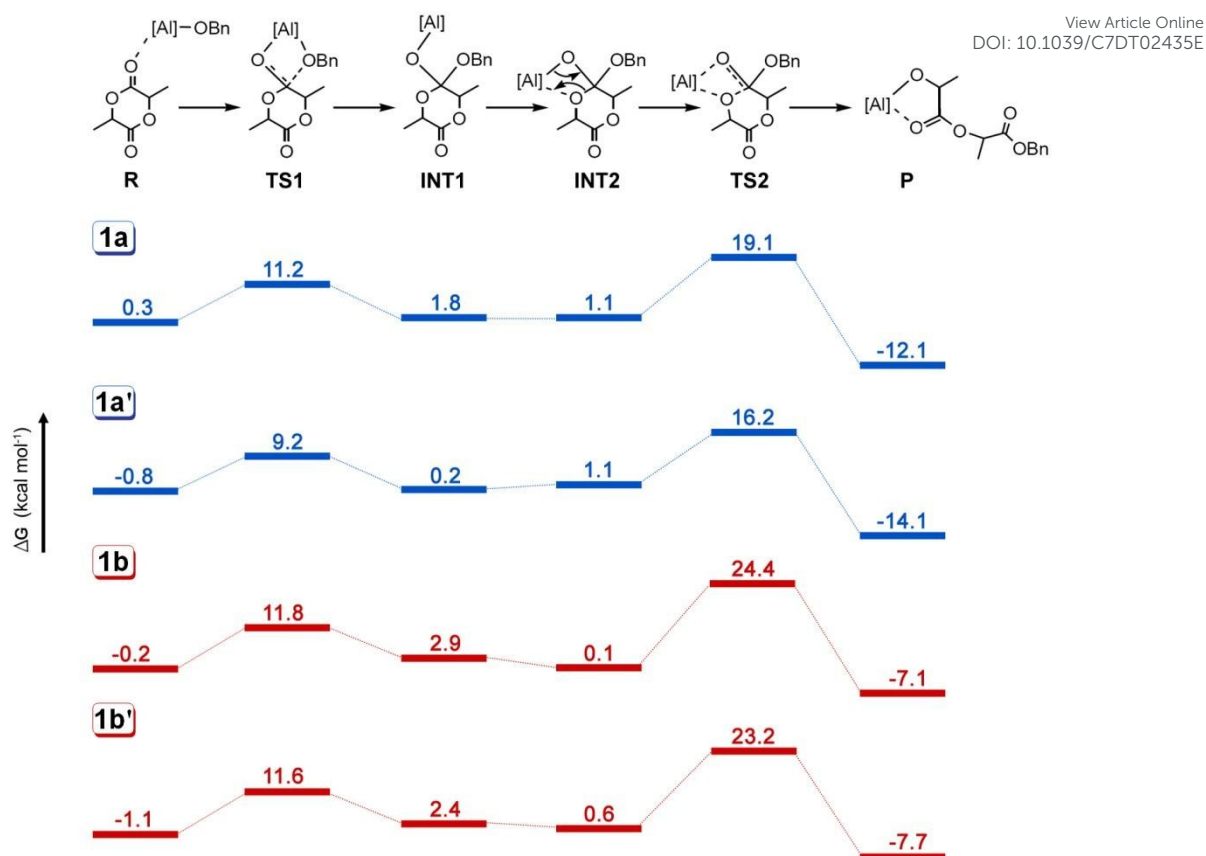


Fig.12 Calculated free energy profiles for the ring-opening insertion of the first *L*-LA monomer by **1a**, **1a'**, **1b**, and **1b'**.

According to the calculated free energy profiles, the ring-opening step is rate-determining in all cases since the Gibbs free energy barrier of the ring-opening transition state (**TS2**) is higher than the insertion transition state (**TS1**). Therefore, we focus primarily on the Gibbs free energies and the optimized structures at **TS2** (Fig. 13). In comparison between four-coordinate and five-coordinate aluminium complexes (**1a** and **1b**; **1a'** and **1b'**), the free energy barriers of four-coordinate complexes, **1a** ($\Delta\Delta G_{\text{TS2}} = +18.0 \text{ kcal mol}^{-1}$) and **1a'** ($\Delta\Delta G_{\text{TS2}} = +15.1 \text{ kcal mol}^{-1}$), are lower than those of five-coordinate counterparts, **1b** ($\Delta\Delta G_{\text{TS2}} = +24.3 \text{ kcal mol}^{-1}$) and **1b'** ($\Delta\Delta G_{\text{TS2}} = +24.0 \text{ kcal mol}^{-1}$), indicating that the ring-opening step of the four-coordinate aluminium complexes is kinetically more favorable. In addition, when comparing the overall reaction energies for the formation of five-membered

metallocyclic product (**P**), the four-coordinate aluminium complexes exhibit lower overall reaction energies than those of the five-coordinate aluminium complexes ($\Delta\Delta G_{\text{Product}} = -12.4$ kcal mol⁻¹ for **1a**; $\Delta\Delta G_{\text{Product}} = -13.3$ kcal mol⁻¹ for **1a'**; $\Delta\Delta G_{\text{Product}} = -6.9$ kcal mol⁻¹ for **1b**; $\Delta\Delta G_{\text{Product}} = -6.6$ kcal mol⁻¹ for **1b'**), suggesting that the products **P** formed by **1a** and **1a'** are thermodynamically more stable than those of **1b** and **1b'**. The calculations were in line with the experimentally observed activities, which indicated that the four-coordinate aluminium complex displayed higher catalytic performance than that of the five-coordinate counterpart.

In the case of four-coordinate aluminium complexes **1a** and **1a'**, the ring-opening step initiated by **1a** proceeds through the higher energy transition state (**TS2**) compared with that of **1a'** ($\Delta G^\ddagger = +19.1$ kcal mol⁻¹ for **1a**; $\Delta G^\ddagger = +16.2$ kcal mol⁻¹ for **1a'**) and the energy barrier of **1a** ($\Delta\Delta G_{\text{TS2}} = +18.0$ kcal mol⁻¹) is also higher than that of **1a'** ($\Delta\Delta G_{\text{TS2}} = +15.1$ kcal mol⁻¹). These findings are consistent with the experimental data that the initiators **1a** has a lower k_{app} value than **1a'** ($k_{\text{app}} = (4.0 \pm 0.1) \times 10^{-5}$ s⁻¹ for **1a**; $k_{\text{app}} = (6.0 \pm 0.1) \times 10^{-5}$ s⁻¹) for **1a'**).⁷⁰ The optimized ring-opening **TS2** structures initiated by **1a** and **1a'** are shown in Figure 12. The presence of the large and less electronegative sulfur atom in the salicylbenzothiazole ligand of **1a** renders the ligand framework more distorted from planarity than for the incorporation of an oxygen atom in the salicylbenzoxazole ligand of **1a'**, as evidenced by a larger observed dihedral angle, N(1)–C(2)–C(3)–C(4), of 20.2° for **1a** and 15.6° for **1a'**. The divergence from planarity of the aromatic system in **1a** reduces the degree of electron delocalization in **1a** compared with **1a'**. Furthermore, the Al–N(1) bond of **1a** (2.140 Å) is found to be longer than that of **1a'** (2.105 Å). The deviation of the dihedral angle from planarity and the observed longer Al–N(1) bond distance in **1a** could be the reasons for the higher energy of **TS2** for **1a**.

Similar observations are also disclosed for the five-coordinate aluminium complexes **1b** and **1b'**. A close examination of the **TS2** geometries of **1b** and **1b'** shown in Fig. 12 revealed that the Al–N(1) bond of **1b** (2.065 Å) is also longer than that of **1b'** (2.011 Å) and

the larger dihedral angle was observed in **1b** (19.7° for **1b** and 13.8° for **1b'**). The ring-opening step of **1b'** ($\Delta\Delta G_{\text{TS2}} = +22.6 \text{ kcal mol}^{-1}$ and $\Delta\Delta G_{\text{Product}} = -6.6 \text{ kcal mol}^{-1}$) is both kinetically and thermodynamically more favorable in comparison with **1b** ($\Delta\Delta G_{\text{TS2}} = +24.3 \text{ kcal mol}^{-1}$ and $\Delta\Delta G_{\text{Product}} = -6.9 \text{ kcal mol}^{-1}$), which is in accord with the higher catalytic activity of **1b'** compared to **1b** ($k_{\text{app}} = (0.54 \pm 0.1) \times 10^{-5} \text{ s}^{-1}$ for **1b** vs. $k_{\text{app}} = (1.7 \pm 0.1) \times 10^{-5} \text{ s}^{-1}$ for **1b'**).⁷⁰

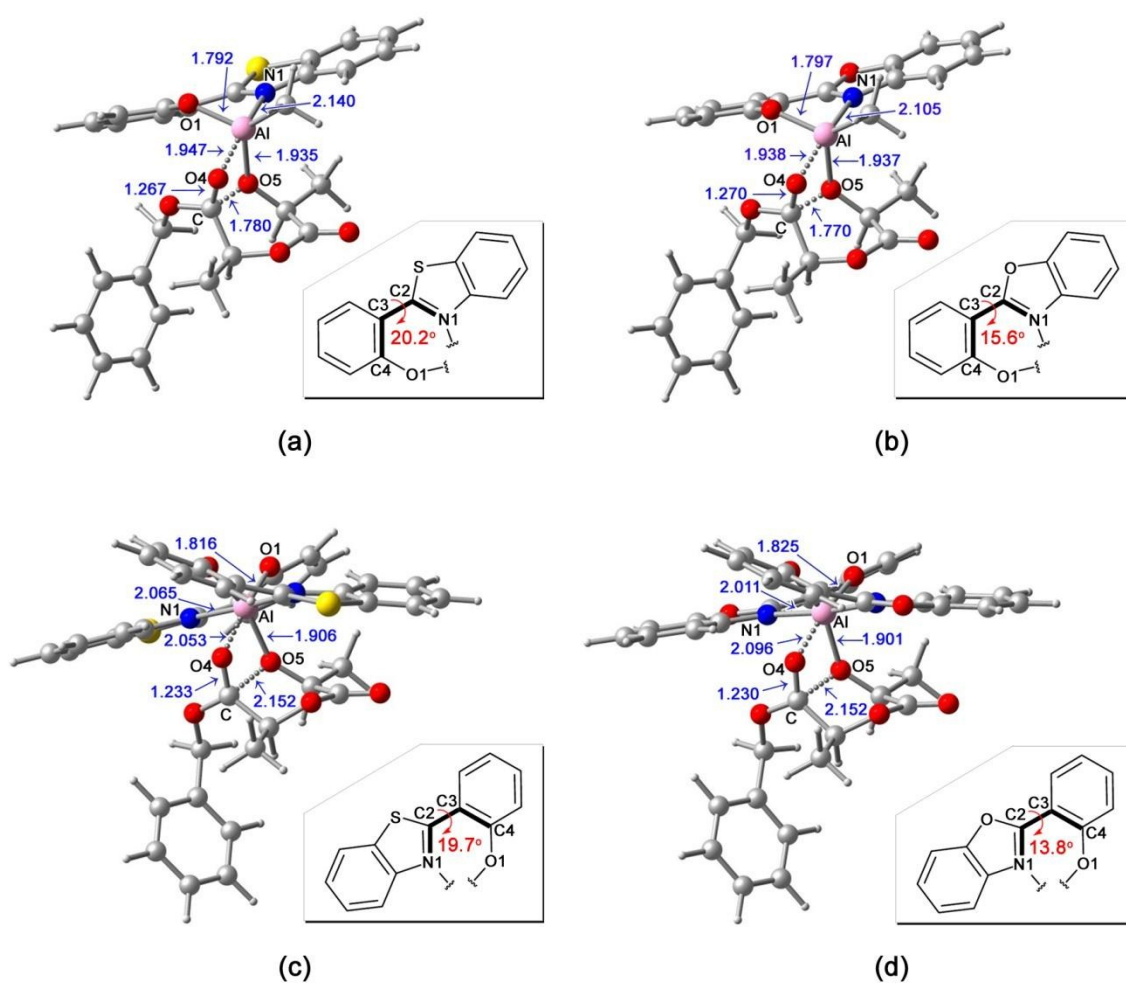


Fig. 13. Optimized ring-opening TS2 structures for the ring-opening polymerisation initiated by (a) **1a**, (b) **1a'**, (c) **1b** and (d) **1b'** (H atoms on the ligand are omitted for clarity: pink = Al; red = O; blue = N; grey = C; yellow = S). Distances are given in Å.

In summary, the studies of the free energy profiles for the ROP of *L*-LA initiated by **1a**, **1a'**, **1b**, and **1b'** provide insights into the different catalytic proficiency of the four-coordinate and the five-coordinate aluminium complexes. Besides, the correlation between geometrical differences and the polymerisation activities was established using the DFT calculations. The calculations also correlate nicely with the experimental data, providing the theoretical supports for the activity observed in the *L*-LA ring-opening polymerisation.

EXPERIMENTAL SECTION

Materials and methods

All the manipulations with air- and water-sensitive compounds were carried out under a dry nitrogen atmosphere using standard Schlenk and cannula techniques in oven-dried glassware or a glove box. Toluene and hexane were distilled from Na–benzophenone and CaH₂ prior to use, respectively. Benzyl alcohol was dried over sodium and then freshly distilled onto activated 4 Å molecular sieves. All the solvents were degassed before use unless stated otherwise. The NMR solvents were dried over 4 Å molecular sieves and degassed prior to use. A 2.0 M solution of trimethylaluminium in toluene (Aldrich) was used without purification. The salicylaldehyde (98%), 3,5-dichlorosalicylaldehyde (99%), 3,5-dibromosalicylaldehyde (98%), *o*-aminothiophenol (99%), and ZrOCl₂·8H₂O (98%) were purchased from Aldrich and used as received. The 3,5-dimethylsalicylaldehyde, 3-phenylsalicylaldehyde and 3,5-di-*tert*-butylsalicylaldehyde were synthesized using a standard method described in the literature.¹³³ The 3-(1,1-diphenylethyl)-5-methylsalicylaldehyde was prepared according to the literature procedure.⁷⁰ *rac*-Lactide (Aldrich) was sublimed three times prior to use. ϵ -Caprolactone (Aldrich) was distilled from CaH₂. All other chemicals are commercially available and were used as received unless otherwise stated. ¹H NMR (399.86 MHz) and ¹³C NMR (100.54 MHz) spectra and the homonuclear decoupled ¹H NMR spectra

were recorded on a Bruker Advance 400 MHz spectrometer at 298 K. The ^1H NMR spectra were referenced internally to the residual proton impurity peaks according to the literature.¹³⁴ Mass spectra were acquired by MALDI-TOF (matrix-assisted laser desorption and ionization time-of-flight) mass spectrometry using a Bruker Daltonics Autoflex speedTM mass spectrometer, equipped with laser frequency at 2000 Hz. Solutions of *trans*-2-[3-(4-*tert*-butylphenyl)-2-methyl-2-propylidene]malonitrile (DCTB) as a matrix (80 μL of a 40 gL^{-1} THF solution), sodium iodide as a cationization agent (20 μL of a 5 gL^{-1} THF solution) and polymer (20 μL of a 1 gL^{-1} THF solution) were mixed together before handed spot to the target followed by solvent evaporation to prepare a thin matrix/polymer film. The samples were measured in linear positive mode and calibrated by comparison to 5 and 20 $\text{kg}\cdot\text{mol}^{-1}$ protein calibration standards I. Elemental analysis data (C, H, and N) were obtained using a Thermo ScientificTM FLASHTM 2000 Organic Elemental Analyzer. Gel permeation chromatography (GPC) measurements were conducted on a Polymer Laboratories PL-GPC-220 instrument equipped with PLgel 5 μm MIXED-D 300 \times 7.5 mm columns and tetrahydrofuran (THF) was used as an eluent (flow rate: 1 mL min^{-1} at 40 $^\circ\text{C}$). The number-average molecular weights (M_n) and polydispersity indices (M_w/M_n) were calibrated against polystyrene (PS) standards.

General Protocol for the Synthesis of Ligands HL^1 – HL^3 .

The reaction was performed according to the procedure previously reported in the literature.⁷⁵ The following example is typical. To a stirred solution of salicylaldehyde (18.77 mmol) in ethanol (20 mL) was slowly added *o*-aminothiophenol (2.00 mL, 18.77 mmol). The reaction mixture was stirred at 80 $^\circ\text{C}$ for 8 h. After cooling to -20 $^\circ\text{C}$, the product was obtained as light yellow crystals.

2-(2'-hydroxyphenyl)benzothiazole (HL¹). Yield: 2.88 g, 77%. ¹H NMR (399.86 MHz, CDCl₃, 298 K): δ 12.51 (br s, 1H, OH), 7.99 (d, ³J_{HH} = 8.1 Hz, 1H, ArH), 7.90 (d, ³J_{HH} = 7.7 Hz, 1H, ArH), 7.70 (dd, ⁴J_{HH} = 1.6 Hz, ³J_{HH} = 7.9 Hz, 1H, ArH), 7.52–7.49 (m, 1H, ArH), 7.43–7.36 (m, 2H, ArH), 7.11 (dd, ⁴J_{HH} = 1.0 Hz, ³J_{HH} = 8.3 Hz, 1H, ArH), 7.00–6.69 (m, 1H, ArH). ¹³C NMR (100.54 MHz, CDCl₃, 298 K): δ 169.4 (C=N), 158.0 (ArC), 151.8 (ArC), 132.8 (ArCH), 132.6 (ArC), 128.4 (ArCH), 126.7 (ArCH), 125.6 (ArCH), 122.1 (ArCH), 121.5 (ArCH), 119.5 (ArCH), 117.9 (ArCH), 116.8 (ArC). Anal. Calcd for C₁₃H₉NOS: C 68.70, H 3.99, N 6.16; found: C 68.75, H 4.00, N 6.56.

2-(2'-hydroxy-3',5'-dimethylphenyl)benzothiazole (HL²). Yield: 1.74 g, 51%. ¹H NMR (399.86 MHz, CDCl₃, 298 K): δ 12.50 (br s, 1H, OH), 7.95 (d, ³J_{HH} = 8.1 Hz, 1H, ArH), 7.88 (d, ³J_{HH} = 8.0 Hz, 1H, ArH), 7.50–7.47 (m, 1H, ArH), 7.40–7.37 (m, 1H, ArH), 7.32 (s, 1H, ArH), 7.07 (s, 1H, ArH), 2.33 (s, 3H, CH₃), 2.32 (s, 3H, CH₃). ¹³C NMR (100.54 MHz, CDCl₃, 298 K): δ 169.8 (C=N), 154.2 (ArC), 151.9 (ArC), 134.9 (ArCH), 132.7 (ArC), 128.1 (ArC), 126.7 (ArC), 126.6 (ArCH), 125.9 (ArCH), 125.3 (ArCH), 122.0 (ArCH), 121.5 (ArCH), 115.6 (ArC), 20.5 (CH₃), 16.0 (CH₃). Anal. Calcd for C₁₅H₁₃NOS: C 70.56, H 5.13, N 5.49; found: C 70.47, H 5.13, N 5.57.

2-(2'-hydroxy-3',5'-dichlorophenyl)benzothiazole (HL³). Yield: 1.64 g, 53%. ¹H NMR (399.86 MHz, CDCl₃, 298 K): δ 13.33 (br s, 1H, OH), 7.99 (d, ³J_{HH} = 7.9 Hz, 1H, ArH), 7.92 (d, ³J_{HH} = 7.8 Hz, 1H, ArH), 7.56 (d, ⁴J_{HH} = 2.4 Hz, 1H, ArH), 7.54–7.52 (m, 1H, ArH), 7.48–7.46 (m, 1H, ArH), 7.44 (d, ⁴J_{HH} = 2.4 Hz, 1H, ArH). ¹³C NMR (100.54 MHz, CDCl₃, 298 K): δ 167.2 (C=N), 152.7 (ArC), 151.2 (ArC), 132.7 (ArC), 132.3 (ArCH), 127.2 (ArCH), 126.4 (ArCH), 126.0 (ArCH), 123.9 (ArC), 123.6 (ArC), 122.5 (ArCH), 121.7 (ArCH), 118.2 (ArC). Anal. Calcd for C₁₃H₇NOSCl₂: C 52.72, H 2.38, N 4.73; found: C 52.59, H 4.90, N 4.61.

General Protocol for the Synthesis of Ligands HL⁴–HL⁷.

The reaction was performed according to the procedure previously reported in the literature.¹⁰⁴ The following example is typical. To a stirred solution of 3,5-dibromosalicylaldehyde (10.47 mmol) in ethanol (10 mL) was slowly added a solution of *o*-aminothiophenol (10.47 mmol) in ethanol (10 mL). The reaction mixture was stirred at room temperature for 30 min, the oxidation cyclization was then carried out by the addition of ZrOCl₂·8H₂O (1.43 mmol). The reaction mixture was further stirred at 80 °C for 24 h and then cooled to –20 °C. The product was obtained as light yellow crystals.

2-(2'-hydroxy-3',5'-dibromophenyl)benzothiazole (HL⁴). Yield: 1.25 g, 45%. ¹H NMR (399.86 MHz, CDCl₃, 298 K): δ 13.44 (s, 1H, OH), 8.00 (d, ³J_{HH} = 8.0 Hz, 1H, ArH), 7.93 (d, ³J_{HH} = 7.9 Hz, 1H, ArH), 7.75 (s, 2H, ArH), 7.57–7.53 (m, 1H, ArH), 7.49–7.45 (m, 1H, ArH). ¹³C NMR (100.54 MHz, CDCl₃, 298 K): δ 167.1 (C=N), 154.1 (ArC), 151.2 (ArC), 137.8 (ArCH), 132.8 (ArC), 129.7 (ArCH), 127.2 (ArCH), 126.5 (ArCH), 122.6 (ArCH), 121.8 (ArCH), 118.8 (ArC), 112.9 (ArC), 110.9 (ArC). Anal. Calcd for C₁₃H₇NOSBr₂: C 40.55, H 1.83, N 3.64; found: C 40.64, H 1.86, N 3.71.

2-(2'-hydroxy-3',5'-di-*tert*-butylphenyl)benzothiazole (HL⁵). Yield: 2.33 g, 80%. ¹H NMR (399.86 MHz, CDCl₃, 298 K): δ 13.01 (s, 1H, OH), 7.56 (d, ⁴J_{HH} = 2.3 Hz, 1H, ArH) 7.97 (d, ³J_{HH} = 7.7 Hz, 1H, ArH), 7.89 (d, ³J_{HH} = 7.4 Hz, 1H, ArH), 7.45 (d, ⁴J_{HH} = 2.3 Hz, 1H, ArH), 7.51–7.46 (m, 1H, ArH), 7.41–7.37 (m, 1H, ArH), 1.52 (s, 9H, C(CH₃)₃), 1.38 (s, 9H, C(CH₃)₃). ¹³C NMR (100.54 MHz, CDCl₃, 298 K): δ 164.08 (C=N), 158.4 (ArCH), 146.6 (ArC), 140.7 (ArC), 137.2 (ArC), 131.6 (ArC), 128.6 (ArCH), 127.3 (ArCH), 127.4 (ArCH), 127.1 (ArCH), 126.7 (ArC), 118.3 (ArC), 117.7 (ArCH), 35.2 (C(CH₃)₃), 34.2 (C(CH₃)₃), 31.4 (C(CH₃)₃), 29.4 (C(CH₃)₃). Anal. Calcd for C₂₁H₂₅NOS: C 74.29, H 7.42, N 4.13; found: C 74.34, H 7.30, N 3.98.

2-(2'-hydroxy-3'-phenylphenyl)benzothiazole (HL⁶). Yield: 2.44 g, 80%. ¹H NMR (399.86 MHz, CDCl₃, 298 K): δ 13.13 (br s, 1H, OH), 7.93 (t, ³J_{HH} = 9.1 Hz, 2H, ArH), 7.72 (d, ³J_{HH} = 7.6 Hz, 1H, ArH), 7.68 (d, ³J_{HH} = 7.6 Hz, 2H, ArH), 7.47 (d, ³J_{HH} = 7.6 Hz, 2H, ArH), 7.52–7.36 (m, 4H, ArH), 7.04 (t, ³J_{HH} = 7.7 Hz, 1H, ArH). ¹³C NMR (100.54 MHz, CDCl₃, 298 K): δ 169.8 (C=N), 155.4 (ArC), 151.8 (ArC), 132.7 (ArC), 137.9 (ArCH), 133.9 (ArC), 132.8 (ArC), 130.8 (ArCH), 129.6 (ArCH), 128.2 (ArCH), 127.9 (ArCH), 127.4 (ArCH), 126.8 (ArCH), 125.7 (ArCH), 122.2 (ArCH), 121.6 (ArCH), 119.6 (ArCH), 117.1 (ArC). Anal. Calcd for C₁₉H₁₃NOS: C 75.22, H 4.32, N 4.62; found: C 75.11, H 4.26, N 4.53.

2-(2'-(hydroxy-3'-1,1-diphenylethyl-5'-methylphenyl)benzothiazole (HL⁷). Yield: 2.00 g, 75%. ¹H NMR (399.86 MHz, CDCl₃, 298 K): δ 12.82 (s, 1H, OH), 7.90 (d, ³J_{HH} = 7.3 Hz, 1H, ArH), 7.86 (d, ³J_{HH} = 7.5 Hz, 1H, ArH), 7.47–7.43 (m, 2H, ArH), 7.39–7.35 (m, 1H, ArH), 7.33–7.29 (m, 4H, ArH), 7.28 (d, ⁴J_{HH} = 1.3 Hz, 1H, ArH), 7.27–7.19 (m, 6H, ArH), 6.58 (d, ⁴J_{HH} = 2.1 Hz, 1H, ArH), 2.42 (s, 3H, CH₃), 2.22 (s, 3H, CH₃). ¹³C NMR (100.54 MHz, CDCl₃, 298 K): δ 169.8 (C=N), 154.6 (ArC), 151.8 (ArC), 148.3 (ArCH), 137.0 (ArC), 134.8 (ArC), 132.8 (ArC), 128.5 (ArCH), 127.9 (ArCH), 127.3 (ArCH), 127.4 (ArCH), 126.6 (ArCH), 125.9 (ArCH), 125.4 (ArC), 122.0 (ArCH), 121.4 (ArCH), 116.7 (ArC), 52.0 (C), 27.6 (CH₃), 20.9 (CH₃). Anal. Calcd for C₂₈H₂₃NOS: C, 79.78; H, 5.50; N, 3.32; found: C, 79.72; H, 5.61; N, 2.99.

General Protocol for the Synthesis of Aluminium Complexes 1a–7a.

In a typical procedure, to a stirred solution of HL¹ (4.40 mmol) in toluene (30 mL) trimethylaluminium (TMA) (2.20 mL of a 2.0 M solution in toluene, 4.40 mmol) was slowly added at room temperature. The reaction mixture was stirred at room temperature for 1 h. The volatiles were removed under reduced pressure to leave a pale yellow solid, which was then recrystallized in hexane at –20°C. The desired products were obtained as light yellow solids.

L¹AlMe₂ (1a). Yield: 1.11 g, 89%. ¹H NMR (399.86 MHz, CDCl₃, 298 K): δ 7.99 (d, ³J_{HH} = 8.3 Hz, 1H, ArH), 7.90 (d, ³J_{HH} = 7.4 Hz, 1H, ArH), 7.67 (dd, ⁴J_{HH} = 1.7 Hz, ³J_{HH} = 8.0 Hz, 1H, ArH), 7.61–7.57 (m, 1H, ArH), 7.52–7.48 (m, 1H, ArH), 7.45–7.41 (m, 1H, ArH), 7.00 (dd, ⁴J_{HH} = 1.0 Hz, ³J_{HH} = 8.4 Hz, 1H, ArH), 6.84–6.80 (m, 1H, ArH), –0.58 (s, 6H, Al(CH₃)₂). ¹³C NMR (100.54 MHz, CDCl₃, 298 K): δ 174.7 (C=N), 161.4 (ArC), 148.2 (ArC), 136.2 (ArCH), 130.5 (ArCH), 129.7 (ArCH), 127.9 (ArC), 126.6 (ArC), 123.0 (ArCH), 122.0 (ArCH), 119.8 (ArCH), 118.2 (ArCH), 116.6 (ArCH), –9.3 (Al(CH₃)₂). Anal. Calcd for C₁₅H₁₄NOSAl: C 63.59, H 4.98, N 4.94; found: C 63.46, H 4.64, N 4.79.

L²AlMe₂ (2a). Yield: 0.82 g, 67%. ¹H NMR (399.86 MHz, CDCl₃, 298 K): δ 7.97 (d, ³J_{HH} = 8.3 Hz, 1H, ArH), 7.88 (d, ³J_{HH} = 8.0 Hz, 1H, ArH), 7.59–7.55 (m, 1H, ArH), 7.49–7.45 (m, 1H, ArH), 7.29 (s, 1H, ArH), 7.17 (s, 1H, ArH), 2.28 (s, 3H, CH₃), 2.26 (s, 3H, CH₃), –0.61 (s, 6H, Al(CH₃)₂). ¹³C NMR (100.54 MHz, CDCl₃, 298 K): δ 175.2 (C=N), 158.3 (ArC), 148.4 (ArC), 137.9 (ArCH), 131.3 (ArC), 130.7 (ArC), 127.8 (ArCH), 126.6 (ArC), 126.7 (ArCH), 126.2 (ArCH), 121.9 (ArCH), 119.8 (ArCH), 115.3 (ArC), 20.5 (CH₃), 16.8 (CH₃), –9.3 (Al(CH₃)₂). Anal. Calcd for C₁₇H₁₈NOSAl: C 65.57, H 5.83, N 4.50; found: C 65.45, H 5.72, N 4.42.

L³AlMe₂ (3a). Yield: 0.87 g, 71%. ¹H NMR (399.86 MHz, CDCl₃, 298 K): δ 8.00 (d, ³J_{HH} = 8.4 Hz, 1H, ArH), 7.94 (d, ³J_{HH} = 8.0 Hz, 1H, ArH), 7.62 (t, ³J_{HH} = 7.8 Hz, 1H, ArH), 7.57–7.52 (m, 2H, ArH), –0.58 (s, 6H, Al(CH₃)₂). ¹³C NMR (100.54 MHz, CDCl₃, 298 K): δ 167.2 (C=N), 152.7 (ArC), 151.2 (ArC), 132.7 (ArC), 132.3 (ArCH), 127.2 (ArCH), 126.4 (ArCH), 126.0 (ArCH), 123.9 (ArC), 123.6 (ArC), 122.5 (ArCH), 121.7 (ArCH), 118.2 (ArC). Anal. Calcd for C₁₅H₁₄NOSCl₂Al: C 51.15, H 3.43, N 3.98; found: C 51.01, H 3.41, N 3.76.

L⁴AlMe₂ (4a). Yield: 0.92 g, 80%. ¹H NMR (399.86 MHz, CDCl₃, 298 K): δ 8.03 (d, ³J_{HH} = 8.3 Hz, 1H, ArH), 7.95 (d, ³J_{HH} = 8.1 Hz, 1H, ArH), 7.83 (d, ⁴J_{HH} = 2.4 Hz, 1H, ArH), 7.74 (d, ⁴J_{HH} = 2.1 Hz, 1H, ArH), 7.67–7.62 (m, 1H, ArH), 7.58–7.55 (m, 1H, ArH), –0.56 (s, 6H,

Al(CH₃)₂). ¹³C NMR (100.54 MHz, CDCl₃, 298 K): δ 167.2 (C=N), 152.7 (ArC), 151.2 (ArC), 132.7 (ArC), 132.3 (ArCH), 127.2 (ArCH), 126.4 (ArCH), 126.0 (ArCH), 123.9 (ArC), 123.6 (ArC), 122.5 (ArCH), 121.7 (ArCH), 118.2 (ArC). Anal. Calcd for C₁₅H₁₂NOSBr₂Al: C 40.84, H 2.74, N 3.18; found: C 40.74, H 2.50, N 3.31.

L⁵AlMe₂ (5a). Yield: 1.10 g, 94%. ¹H NMR (399.86 MHz, CDCl₃, 298 K): δ 7.95 (d, ³J_{HH} = 8.2 Hz, 1H, ArH), 7.87 (d, ³J_{HH} = 7.7 Hz, 1H, ArH), 7.58–7.54 (m, 2H, ArH), 7.50–7.45 (m, 2H, ArH), 1.46 (s, 9H, C(CH₃)₃), 1.35 (s, 9H, C(CH₃)₃), –0.61 (s, 6H, Al(CH₃)₂). ¹³C NMR (100.54 MHz, CDCl₃, 298 K): δ 176.0 (C=N), 158.9 (ArC), 148.3 (ArC), 141.6 (ArC), 139.6 (ArC), 131.2 (ArCH), 130.6 (ArC), 127.7 (ArCH), 126.2 (ArCH), 123.6 (ArCH), 121.8 (ArCH), 119.6 (ArCH), 116.0 (ArC), 35.7 (C(CH₃)₃), 34.4 (C(CH₃)₃), 31. (C(CH₃)₃), 29.6 (C(CH₃)₃). Anal. Calcd for C₂₃H₃₀NOSAl: C 69.84, H 7.64, N 3.54; found: C 69.73, H 7.77, N 3.56.

L⁶AlMe₂ (6a). Yield: 0.78 g, 66%. ¹H NMR (399.86 MHz, CDCl₃, 298 K): δ 7.97 (d, ³J_{HH} = 8.1 Hz, 1H, ArH), 7.90 (d, ³J_{HH} = 8.0 Hz, 1H, ArH), 7.67 (dd, ⁴J_{HH} = 2.1 Hz, ³J_{HH} = 8.4 Hz, 1H, ArH), 7.65–7.63 (m, 2H, ArH), 7.59–7.55 (m, 1H, ArH), 7.52–7.47 (m, 2H, ArH), 7.44–7.40 (m, 2H, ArH), 7.35–7.31 (m, 1H, ArH), 6.87 (t, ³J_{HH} = 7.7, 1H, ArH), –0.60 (s, 6H, Al(CH₃)₂). ¹³C NMR (100.54 MHz, CDCl₃, 298 K): δ 169.8 (C=N), 155.4 (ArC), 151.8 (ArC), 132.7 (ArC), 137.9 (ArCH), 133.9 (ArC), 132.8 (ArC), 130.8 (ArCH), 129.6 (ArCH), 128.2 (ArCH), 127.9 (ArCH), 127.4 (ArCH), 126.8 (ArCH), 125.7 (ArCH), 122.2 (ArCH), 121.6 (ArCH), 119.6 (ArCH), 117.1 (ArC). Anal. Calcd for C₂₁H₁₃₈NOSAl: C 70.18, H 5.05, N 3.90; found: C 69.98, H 5.16, N 3.72.

L⁷AlMe₂ (7a). Yield: 0.85 g, 75%. ¹H NMR (399.86 MHz, CDCl₃, 298 K): δ 7.85 (t, ³J_{HH} = 7.4 Hz, 2H, ArH), 7.54–7.50 (m, 1H, ArH), 7.46–7.40 (m, 2H, ArH), 7.34–7.27 (m, 4H, ArH), 7.25–7.19 (m, 6H, ArH), 6.87–6.86 (m, 1H, ArH), 2.32 (s, 3H, CH₃), 2.22 (s, 3H, CH₃), –0.90 (s, 6H, Al(CH₃)₂). ¹³C NMR (100.54 MHz, CDCl₃, 298 K): δ 175.0 (C=N), 158.3

(ArC), 148.3 (ArCH), 141.2 (ArC), 137.4 (ArCH), 130.6 (ArC), 128.5 (ArCH), 128.1 (ArC), 127.8 (ArCH), 127.7 (ArC), 126.2 (ArCH), 125.9 (ArCH), 125.6 (ArCH), 125.3 (ArC), 121.8 (ArCH), 119.6 (ArCH), 116.7 (ArC), 52.1 (C), 28.2 (CH₃), 20.9 (CH₃), -9.5 (Al(CH₃)₂).
 Anal. Calcd for C₃₀H₂₈NOSAl: C 75.44, H 5.91, N 2.93; found: C 75.56, H 5.73, N 3.16.

General Protocol for the Synthesis of Aluminium Complexes **1b–7b**.

In a typical procedure, to a stirred solution of **HL**¹ (4.40 mmol) in toluene (30 mL) trimethylaluminium (TMA) (1.10 mL of a 2.0 M solution in toluene, 2.20 mmol) was slowly added at room temperature. The reaction mixture was stirred at 100 °C for 24 h. After cooling to room temperature, a solid precipitated. The desired products were obtained as light yellow solids.

L¹₂AlMe (**1b**). Yield: 0.93 g, 85%. ¹H NMR (399.86 MHz, CDCl₃, 298 K): δ 8.34 (d, ³J_{HH} = 8.3 Hz, 2H, ArH), 7.81 (d, ³J_{HH} = 7.8 Hz, 2H, ArH), 7.68 (dd, ⁴J_{HH} = 1.5 Hz, ³J_{HH} = 7.9 Hz, 2H, ArH), 7.46–7.42 (m, 2H, ArH), 7.38–7.34 (m, 2H, ArH), 7.26–7.24 (m, 2H, ArH), 6.78–6.73 (m, 4H, ArH), -0.78 (s, 3H, AlCH₃). ¹³C NMR (100.54 MHz, CDCl₃, 298 K): δ 171.5 (C=N), 160.8 (ArC), 150.7 (ArC), 134.5 (ArCH), 131.6 (ArC), 129.4 (ArCH), 128.4 (ArC), 126.6 (ArC), 125.7 (ArCH), 123.4 (ArCH), 122.5 (ArCH), 121.3 (ArCH), 118.0 (ArCH), -5.86 Al(CH₃). Anal. Calcd for C₂₇H₁₉N₂O₂S₂Al: C 65.57, H 3.87, N 5.66; found: C 65.30, H 3.95, N 5.53.

L²₂AlMe (**2b**). Yield: 0.61 g, 57%. ¹H NMR (399.86 MHz, CDCl₃, 298 K): δ 8.45 (d, ³J_{HH} = 7.4 Hz, 2H, ArH), 7.87 (d, ³J_{HH} = 7.4 Hz, 2H, ArH), 7.47–7.38 (m, 6H, ArH), 7.02 (s, 2H, ArH), 2.28 (s, 6H, (CH₃)₂), 1.76 (m, 6H, (CH₃)₂), -0.55 (s, 3H, AlCH₃). ¹³C NMR (100.54 MHz, CDCl₃, 298 K): δ 171.8 (C=N), 157.59 (ArC), 150.8 (ArC), 136.3 (ArCH), 131.5 (ArC), 130.9 (ArC), 126.5 (ArCH), 126.7 (ArC), 126.1 (ArCH), 125.5 (ArCH), 124.0

(ArCH), 121.1 (ArCH), 116.6 (ArC), 20.6 (CH₃), 17.0 (CH₃), -11.5 (AlCH₃). Anal. Calcd for C₃₁H₂₇N₂O₂S₂Al: C 67.61, H 4.94, N 5.09; found: C 67.63, H 4.84, N 5.35.

L³₂AlMe (3b). Yield: 0.56 g, 52%. ¹H NMR (399.86 MHz, CDCl₃, 298 K): δ 8.48 (d, ³J_{HH} = 8.2 Hz, 2H, ArH), 7.91 (d, ³J_{HH} = 7.7 Hz, 2H, ArH), 7.65 (d, ⁴J_{HH} = 2.5 Hz, 2H, ArH), 7.56–7.47 (m, 4H, ArH), 7.40 (d, ⁴J_{HH} = 2.5 Hz, 2H, ArH), -0.52 (s, 3H, AlCH₃). ¹³C NMR (100.54 MHz, CDCl₃, 298 K): δ 162.4 (C=N), 158.8 (ArC), 150.3 (ArC), 135.5 (ArCH), 131.3 (ArC), 127.9 (ArC), 126.8 (ArCH), 126.7 (ArCH), 126.5 (ArCH), 124.9 (ArCH), 121.8 (ArC), 121.1 (ArCH), 119.4 (ArC), -8.9 (AlCH₃). Anal. Calcd for C₂₇H₁₅N₂O₂S₂Cl₄Al: C 51.28, H 2.39, N 4.43; found: C 51.53, H 2.44, N 4.62.

L⁴₂AlMe (4b). Yield: 0.68 g, 65%. ¹H NMR (399.86 MHz, CDCl₃, 298 K): δ 8.49 (d, ³J_{HH} = 8.3 Hz, 2H, ArH), 7.91 (d, ³J_{HH} = 7.9 Hz, 2H, ArH), 7.65 (d, ⁴J_{HH} = 2.5 Hz, 2H, ArH), 7.56–7.47 (m, 4H, ArH), 7.40 (d, ⁴J_{HH} = 2.5 Hz, 2H, ArH), -0.52 (s, 3H, AlCH₃). ¹³C NMR (100.54 MHz, CDCl₃, 298 K): δ 169.0 (C=N), 156.1 (ArC), 150.3 (ArC), 139.0 (ArCH), 131.3 (ArC), 130.5 (ArCH), 126.7 (ArCH), 126.5 (ArCH), 125.2 (ArCH), 121.1 (ArCH), 119.8 (ArC), 118.2 (ArC), 108.8 (ArC), -8.4 (AlCH₃). Anal. Calcd for C₂₇H₁₅N₂O₂S₂Br₄Al: C 40.03, H 1.87, N 3.46; found: C 40.22, H 1.87, N, 3.58.

L⁵₂AlMe (5b). Yield: 0.55 g, 52%. ¹H NMR (399.86 MHz, CDCl₃, 298 K): δ 8.50 (d, ³J_{HH} = 7.9 Hz, 2H, ArH), 7.88 (d, ³J_{HH} = 7.8 Hz, 2H, ArH), 7.56 (d, ⁴J_{HH} = 2.5 Hz, 2H, ArH), 7.50–7.40 (m, 4H, ArH), 7.35 (d, ⁴J_{HH} = 2.5 Hz, 2H, ArH), 1.31 (s, 18H, C(CH₃)₃), 0.88 (s, 18H, C(CH₃)₃), -0.57 (s, 3H, AlCH₃). ¹³C NMR (100.54 MHz, CDCl₃, 298 K): δ 173.3 (C=N), 158.0 (ArC), 150.8 (ArC), 140.7 (ArCH), 139.1 (ArCH), 131.5 (ArC), 129.5 (ArC), 126.0 (ArCH), 125.3 (ArCH), 124.5 (ArCH), 123.8 (ArCH), 120.8 (ArC), 117.3 (ArC), 34.9 (C(CH₃)₃), 34.2 (C(CH₃)₃), 31.5 (C(CH₃)₃), 29.2 (C(CH₃)₃), -1.7 (AlCH₃). Anal. Calcd for C₄₃H₅₁N₂O₂S₂Al: C 71.83, H 7.15, N 3.90; found: C 71.79, H 7.18, N 3.53.

L⁶₂AlMe (6b). Yield: 0.48 g, 45%. ¹H NMR (399.86 MHz, CDCl₃, 298 K): δ 7.85 (dd, ⁴J_{HH} = 1.7 Hz, ³J_{HH} = 8.0 Hz, 2H, ArH), 7.74 (d, ³J_{HH} = 8.6 Hz, 4H, ArH), 7.44 (dd, ⁴J_{HH} = 1.7 Hz, ³J_{HH} = 7.3 Hz, 2H, ArH), 7.27–7.25 (m, 4H, ArH), 7.20–7.16 (m, 2H, ArH), 6.94 (t, ³J_{HH} = 7.7 Hz, 2H, ArH), 6.89–6.85 (m, 2H, ArH), 6.69–6.65 (m, 6H, ArH), –0.66 (s, 3H, AlCH₃). ¹³C NMR (100.54 MHz, CDCl₃, 298 K): δ 175.0 (C=N), 159.0 (ArC), 148.4 (ArC), 138.4 (ArC), 136.8 (ArCH), 134.6 (ArC), 130.7 (ArC), 129.6 (ArCH), 129.2 (ArCH), 128.1 (ArCH), 127.9 (ArCH), 127.1 (ArCH), 126.6 (ArCH), 122.0 (ArCH), 119.9 (ArCH), 118.1 (ArCH), 117.4 (ArC), –9.34 (AlCH₃). Anal. Calcd for C₃₉H₂₇N₂O₂S₂Al: C 72.43, H 4.21, N 4.33; found: C 72.29, H 4.31, N 4.56.

L⁷₂AlMe (7b). Yield: 0.86 g, 41%. ¹H NMR (399.86 MHz, CDCl₃, 298 K): δ 7.91 (d, ³J_{HH} = 8.4 Hz, 2H, ArH), 7.76 (d, ³J_{HH} = 7.9 Hz, 2H, ArH), 7.38 (s, 2H, ArH), 7.31 (t, ³J_{HH} = 7.6 Hz, 2H, ArH), 7.22 (t, ³J_{HH} = 8.0 Hz, 2H, ArH), 7.08–7.00 (m, 6H, ArH), 6.88 (d, ³J_{HH} = 6.8 Hz, 4H, ArH), 6.71–6.60 (m, 6H, ArH), 6.64–6.62 (m, 4H, ArH), 6.43 (s, 1H, ArH), 2.17 (s, 3H, CH₃), 1.93 (s, 3H, CH₃), –0.66 (s, 3H, AlCH₃). ¹³C NMR (100.54 MHz, CDCl₃, 298 K): δ 171.9 (C=N), 157.6 (ArC), 150.2 (ArC), 149.4 (ArC), 148.0 (ArC), 140.1 (ArC), 137.0 (ArC), 131.1 (ArC), 129.1 (ArCH), 128.5 (ArCH), 127.7 (ArCH), 127.1 (ArCH), 127.0 (ArCH), 125.6 (ArCH), 125.5 (ArCH), 125.2 (ArCH), 125.1 (ArCH), 125.0 (ArCH), 124.2 (ArCH), 120.5 (ArCH), 118.6 (ArC), 52.0 (C), 26.7 (CH₃), 20.9 (CH₃). Anal. Calcd for C₅₇H₄₇N₂O₂S₂Al: C 77.52, H 5.36, N 3.11; found: C 77.31, H 5.42, N 3.10.

General Polymerisation Procedure for *rac*-LA

In a nitrogen-filled glove box, *rac*-lactide (720 mg, 5.0 mmol) and benzyl alcohol (5.17 μL, 0.05 mmol) were placed in a polymerisation ampoule. To this ampoule was added a solution of initiator (0.05 mmol) in toluene (6.00 mL) ([monomer]:[Al] = 100:1). The reaction was stirred for the desired reaction time at 70 °C. Subsequently, the reaction was quenched with

methanol (2-3 drops). The polymer was precipitated from excess methanol, collected by filtration and dried *in vacuo* to a constant mass. Conversions were determined by integration of the monomer versus polymer methine resonances in the ^1H NMR spectrum of crude product (in CDCl_3).

General Polymerisation Procedure for ϵ -CL

In a nitrogen-filled glove box, ϵ -caprolactone (570 mg, 5.0 mmol) and benzyl alcohol (5.17 μL , 0.05 mmol) were placed in a polymerisation ampoule. To this ampoule was added a solution of initiator (0.05 mmol) in toluene (3.00 mL) ([monomer]:[Al] = 100:1). The reaction was stirred for the desired reaction time at 70 $^\circ\text{C}$. At the desired reaction time, the reaction was quenched with methanol (2-3 drops). The polymer was precipitated from excess methanol, collected by filtration and dried *in vacuo* to a constant mass. Conversions were determined by integration of the monomer versus polymer methylene resonances in the ^1H NMR spectrum of crude product (in CDCl_3).

General Procedure for Kinetic Studies

The *rac*-LA polymerisations were carried out at 70 $^\circ\text{C}$ in a glove box. The molar ratio of monomer to initiator was fixed at 50:1. At appropriate time intervals, 0.5 μL aliquots were removed and quenched with methanol. The solvent was removed *in vacuo* and the percent conversion was determined by ^1H NMR in CDCl_3 .

Crystal Structure Determination

The diffraction data were collected on a Bruker APEXII CCD diffractometer controlled by APEX3 software and the cell refinement, and data reduction was carried out by SAINT.¹³⁵ The measuring temperature was 100 K (under the flow of liquid nitrogen). Absorption

correction was done by multi-scan method using SADABS.¹³⁶ The crystal was kept at 100 K during data collection. Using Olex2,¹³⁷ the structure was solved with the ShelXT structure solution program using Intrinsic Phasing and refined with the ShelXL refinement package using Least Squares minimization.¹³⁸ All non-hydrogen atoms were treated anisotropically while the H atoms were treated by a constrained refinement. The software package used to prepare molecular graphics and materials for publication was Mercury.¹³⁹ Crystallographic data have been deposited at the Cambridge Crystallographic Data Centre under reference numbers CCDC 1551251 (**5a**) and 1551250 (**1b**).

Computational details

All geometry optimizations were carried out in the gas phase without molecular symmetry constraints using the hybrid meta exchange-correlation functional with double the amount of nonlocal exchange¹²⁹⁻¹³¹ (M06-2X) level of theory as implemented in the Gaussian09 program package.¹²⁸ The standard all-electron Pople basis set 6-311G(d,p) was applied to all atoms in the systems.¹³² Frequency analysis was conducted at the same level of theory to verify that the optimized transition states were located at saddle points, signifying that the transition states possessed only one imaginary vibrational frequency corresponding to the relevant reaction coordinate. Gibbs free energies were calculated using the ideal gas, rigid rotor harmonic oscillator approximations at the temperature of 343.15 K.

CONCLUSIONS

Two series of aluminium complexes supported by bidentate salicylbenzothiazole ligands were successfully synthesized and characterized. All the complexes were efficient initiators for the ROP of *rac*-lactide and ϵ -caprolactone, affording polymers with predicted molecular weights and narrow molecular weight distributions. Four-coordinate aluminium complexes

were acted as “immortal polymerisation” catalysts when more than one equivalent of benzyl alcohol was employed. Kinetic studies revealed that the polymerisations promoted by all complexes were first order in the monomer conversion. End group analysis by ^1H NMR spectroscopy and MALDI-TOF Mass Spectrometry supported a coordination-insertion mechanism. The geometry around the aluminium center and the phenoxy substituents had effects on both catalytic activity and stereoselectivity.

In comparison to aluminium salicylbenzoxazole complexes, the lower degree of polymerisation control regarding activity and selectivity in *rac*-LA polymerisations were observed when employing aluminium salicylbenzothiazole complexes. The highest isotactic PLA with the P_m value of 0.70 was produced by **7a** at 50 °C, and **1a** exhibited the highest catalytic activity. Detailed DFT studies unveiled the different catalytic activities between two catalytic systems and the calculations were in good agreement with the experimental data. Finally, we believe that the work reported herein will be beneficial in future catalyst design, especially for the metal complexes bearing bidentate ligands.

ACKNOWLEDGEMENTS

We gratefully acknowledge the financial support from Kasetsart University Research and Development Institute (KURDI) (Grant no. 105.60) and National Research Council of Thailand (NRCT). This research is also supported in part by the Graduate Program Scholarship from the Graduate School, Kasetsart University (C.N.). Assoc. Prof. Khamphree Phomphrai at Vidyasirimedhi Institute of Science and Technology (VISTEC) is acknowledged for the MALDI-TOF MS analysis. P.H. and P.C. thank Kasetsart University and the Center of Excellence for Innovation in Chemistry (PERCH-CIC), the Office of the Higher Education Commission, Ministry of Education for financial support.

REFERENCES

- [1] R. E. Drumright, P. R. Gruber and D. E. Henton, *Adv. Mater.*, 2000, **12**, 1841–1846.
- [2] A. J. Ragauskas, C. K. Williams, B. H. Davison, G. Britovsek, J. Cairney, C. A. Eckert, W. J. Frederick, J. P. Hallett, D. J. Leak, C. L. Liotta, J. R. Mielenz, R. Murphy, R. Templer and T. Tschaplinski, *Science.*, 2006, **311**, 484–489.
- [3] S. Slomkowski, S. Penczek and A. Duda, *Polym. Adv. Technol.*, 2014, **25**, 436–447.
- [4] R. Auras, B. Harte and S. Selke, *Macromol. Biosci.*, 2004, **4**, 835–864.
- [5] Y. Ikada, K. Jamshidi, H. Tsuji and S. H. Hyon, *Macromolecules*, 1987, **20**, 904–906.
- [6] H. Tsuji, *Adv. Drug. Delivery Rev.*, 2016, **107**, 97–135.
- [7] R. H. Platel, L. M. Hodgson and C. K. Williams, *Polym. Rev.*, 2008, **48**, 11–63.
- [8] C. A. Wheaton, P. G. Hayes and B. J. Ireland, *Dalton Trans.*, 2009, 4832–4846.
- [9] C. M. Thomas, *Chem. Soc. Rev.*, 2010, **39**, 165–173.
- [10] M. J. Stanford and A. P. Dove, *Chem. Soc. Rev.*, 2010, **39**, 486–494.
- [11] P. J. Dijkstra, H. Du and J. Feijen, *Polym. Chem.*, 2011, **2**, 520–527.
- [12] A. Sauer, A. Kapelski, C. Fliedel, S. Dagorne, M. Kol and J. Okuda, *Dalton Trans.*, 2013, **42**, 9907–9023.
- [13] S. M. Guillaume, E. Kirillov, Y. Sarazin and J.-F. Carpentier, *Chem. Eur. J.*, 2015, **21**, 7988–8003.
- [14] E. Le Roux, *Coord. Chem. Rev.*, 2016, **306**, 65–85.
- [15] G. Li, M. Lamberti, D. Pappalardo and C. Pellecchia, *Macromolecules*, 2012, **45**, 8614–8620.
- [16] C. Bakewell, R. H. Platel, S. K. Cary, S. M. Hubbard, J. M. Roaf, A. C. Levine, A. J. P. White, N. J. Long, M. Haaf and C. K. Williams, *Organometallics*, 2012, **31**, 4729–4736.

- [17] W. Yang, K.-Q. Zhao, T. J. Prior, D. L. Hughes, A. Arbaoui, M. R. J. Elsegood and C. Redshaw, *Dalton Trans.*, 2016, **45**, 11990–12005. View Article Online
DOI: 10.1039/C7DT02435E
- [18] W. Zhang, Y. Wang, L. Wang, C. Redshaw and W.-H. Sun, *J. Organomet. Chem.*, 2014, **750**, 65–73.
- [19] S. Tabthong, T. Nanok, P. Sumrit, P. Kongsaree, S. Prabpai, P. Chuawong and P. Hormnirun, *Macromolecules*, 2015, **48**, 6846–6861.
- [20] P. Horeglad, O. Ablialimov, G. Szczepaniak, A. M. Dabrowska, M. Dranka and J. Zachara, *Organometallics*, 2014, **33**, 100–111.
- [21] A. B. Kremer, R. J. Andrews, M. J. Milner, X. R. Zhang, T. Ebrahimi, B. O. Patrick, P. L. Diaconescu and P. Mehrkhodavandi, *Inorg. Chem.*, 2017, **56**, 1375–1385.
- [22] A. Thevenon, C. Romain, M. S. Bennington, A. J. P. White, H. J. Davidson, S. Brooker and C. K. Williams, *Angew. Chem. Int. Ed.*, 2016, **55**, 8680–8685.
- [23] T. Rosen, Y. Popowski, I. Goldberg and M. Kol, *Chem. Eur. J.*, 2016, **22**, 11533–11536.
- [24] D. Jędrzkiewicz, G. Adamus, M. Kwiecień, Ł. John and J. Ejfler, *Inorg. Chem.*, 2017, **56**, 1349–1365.
- [25] H. Xie, Z. Mou, B. Liu, P. Li, W. Rong, S. Li and D. Cui, *Organometallics*, 2014, **33**, 722–730.
- [26] T. Rosen, I. Goldberg, V. Venditto, M. Kol, *J. Am. Chem. Soc.*, 2016, **138**, 12041–12044.
- [27] S. M. Quan and P. L. Diaconescu, *Chem. Commun.*, 2015, **51**, 9643–9646.
- [28] A. B. Kremer, K. M. Osten, I. Yu, T. Ebrahimi, D. C. Aluthge and P. Mehrkhodavandi, *Inorg. Chem.*, 2016, **55**, 5365–5374.
- [29] M. Cybukarczyk, M. Dranka, J. Zachara and P. Horeglad, *Organometallics*, 2016, **35**, 3311–3322.

- [30] J.-C. Buffet, A. N. Marin, M. Kol and J. Okuda, *Polym. Chem.*, 2011, **2**, 2378–2384. View Article Online
DOI: 10.1039/C7DT02435E
- [31] C. Bakewell, A. J. P. White, N. J. Long and C. K. Williams, *Angew. Chem. Int. Ed.*, 2014, **53**, 9226–9230.
- [32] R. Lapenta, A. Buonerba, A. De Nisi, M. Monari, A. Grassi, S. Milione and C. Capacchione, *Inorg. Chem.*, 2017, **56**, 3447–3458.
- [33] Y. Wei, S. Wang and S. Zhou, *Dalton Trans.*, 2016, **45**, 4471–4485.
- [34] P. Hormnirun, E. L. Marshall, V. C. Gibson, R. I. Pugh and A. J. P. White, *Proc. Natl. Acad. Sci. U. S. A.*, 2006, **103**, 15343–15348.
- [35] N. Nomura, R. Ishii, Y. Yamamoto and T. Kondo, *Chem. Eur. J.*, 2007, **13**, 4433–4451.
- [36] E. E. Marlier, J. A. Macaranas, D. J. Marell, C. R. Dunbar, M. A. Johnson, Y. DePorre, M. O. Miranda, B. D. Neisen, C. J. Cramer, M. A. Hillmyer and W. B. Tolman, *ACS Catal.*, 2016, **6**, 1215–1224.
- [37] C. Kan, J. Ge and H. Ma, *Dalton Trans.*, 2016, **45**, 6682–6695.
- [38] P. Hormnirun, E. L. Marshall, V. C. Gibson, A. J. P. White and D. J. Williams, *J. Am. Chem. Soc.*, 2004, **126**, 2688–2689.
- [39] H. Du, A. H. Velders, P. J. Dijkstra, J. Sun, Z. Zhong, X. Chen and J. Feijen, *Chem. Eur. J.*, 2009, **15**, 9836–9845.
- [40] Y. Wang and H. Ma, *Chem. Commun.*, 2012, **48**, 6729–6731.
- [41] P. Sumrit and P. Hormnirun, *Macromol. Chem. Phys.*, 2013, **214**, 1845–1851.
- [42] K. Press, I. Goldberg and M. Kol, *Angew. Chem. Int. Ed.*, 2015, **54**, 14858–14861.
- [43] P. McKeown, M. G. Davidson, G. Kociok-Köhn and M. D. Jones, *Chem. Comm.*, 2016, **52**, 10431–10434.
- [44] E. L. Whitelaw, G. Lorain, M. F. Mahon and M. D. Jones, *Dalton Trans.*, 2011, **40**, 11469–11473.

- [45] I. dos Santos Vieira, E. L. Whitelaw, M. D. Jones and S. Herres-Pawlis, *Chem. Eur. J.*, 2013, **19**, 4712–4716. View Article Online
DOI: 10.1039/C7DT02435E
- [46] A. Pilone, K. Press, I. Goldberg, M. Kol, M. Mazzeo and M. Lamberti, *J. Am. Chem. Soc.*, 2014, **136**, 2940–2943.
- [47] S. M. Kirk, G. Kociok-Köhn and M. D. Jones, *Organometallic*, 2016, **35**, 3837–3843.
- [48] N. Nomura, T. Aoyama, R. Ishii and T. Kondo, *Macromolecules*, 2005, **38**, 5363–5366.
- [49] J. Liu, N. Iwasa and K. Nomura, *Dalton Trans.*, 2008, 3978–3988.
- [50] D. Pappalardo, L. Annunziata and C. Pellicchia, *Macromolecules*, 2009, **42**, 6056–6062.
- [51] W. Zhang, Y. Wang, W.-H. Sun, L. Wang and C. Redshaw, *Dalton Trans.*, 2012, **41**, 11587–11596.
- [52] A. Meduri, T. Fuoco, M. Lamberti, C. Pellicchia and D. Pappalardo, *Macromolecules*, 2014, **47**, 534–543.
- [53] Y. Wang and H. Ma, *J. Organomet. Chem.*, 2013, **731**, 23–28.
- [54] S. J. Roymuhury, D. Chakraborty and V. Ramkumar, *Eur. Polym. J.*, 2015, **70**, 203–214.
- [55] S. Gong and H. Ma, *Dalton Trans.*, 2008, 3345–3357.
- [56] W. Yai, Y. Mu, A. Gao, W. Gao and L. Ye, *Dalton Trans.*, 2008, 3199–3206.
- [57] D. Li, Y. Peng, C. Geng, K. Liu and D. Kong, *Dalton Trans.*, 2013, **42**, 11295–11303.
- [58] D.-R. Dauer and D. Stalke, *Dalton Trans.*, 2014, **43**, 14432–14439.
- [59] F. Qian, K. Liu and H. Ma, *Dalton Trans.*, 2010, **39**, 8071–8083.
- [60] S. Tabthong, T. Nanok, P. Kongsaree, S. Prabpai and P. Hormnirun, *Dalton Trans.*, 2014, **43**, 1348–1359.

- [61] S. Pracha, S. Praban, A. Niewpung, G. Kotpisan, P. Kongsaree, S. Saitong, T. Khamnaen, P. Phiriyawirut, S. Charoenchaidet and K. Phomphrai, *Dalton Trans.*, 2013, **42**, 15191–15198. View Article Online
DOI: 10.1039/C7DT02435E
- [62] C. Zhang and Z.-X. Wang, *J. Organomet. Chem.*, 2008, **693**, 2151–3158.
- [63] W. Yao, Y. Mu, A. Gao, Q. Su, Y. Liu and Y. Zhang, *Polymer*, 2008, **49**, 2486–2491.
- [64] X. Wang, K.-Q. Zhao, Y. Al-Khafaji, S. Mo, T. J. Prior, M. R. J. Elsegood and C. Redshaw, *Eur. J. Inorg. Chem.*, 2017, 1951–1965.
- [65] N. Iwasa, M. Fujiki, M. and K. Nomura, *J. Mol. Catal. A: Chem.*, 2008, **292**, 67–75.
- [66] N. Iwasa, J. Liu and K. Nomura, *Catal. Commun.*, 2008, **9**, 1148–1152.
- [67] A. Arbaoui, C. Redshaw and D. L. Hughes, *Chem. Commun.*, 2008, 4717–4719.
- [68] W.-H. Sun, M. Shen, W. Zhang, W. Huang, S. Liu and C. Redshaw, *Dalton Trans.*, 2011, **40**, 2645–2653.
- [69] A. Arbaoui and C. Redshaw, *Polym. Chem.*, 2010, **1**, 801–826.
- [70] P. Sumrit, P. Chuawong, T. Nanok, T. Duangthongyou and P. Hormnirun, *Dalton Trans.*, 2016, **45**, 9250–9266.
- [71] E. Y. Tshuva, S. Groysman, I. Goldberg and M. Kol, *Organometallics*, 2002, **21**, 662–670.
- [72] X.-C. Shi and G.-X. Jin, *Dalton Trans.*, 2011, **40**, 11914–11919.
- [73] M.-C. Chang, W.-Y. Lu, H.-Y. Chang, Y.-C. Lai, M. Y. Chiang, H.-Y. Chen and H.-Y. Chen, *Inorg. Chem.*, 2015, **54**, 11292–11298.
- [74] Y.-T. Huang, W.-C. Wang, C.-P. Hsu, W.-Y. Lu, W.-J. Chuang, M. Y. Chiang, Y.-C. Lai and H.-Y. Chen, *Polym. Chem.*, 2016, **7**, 4367–4377.
- [75] A.-Q. Jia and G.-X. Jin, *Dalton Trans.*, 2009, 8838–8845.
- [76] F. M. Moghaddam, H. Ismaili and G. R. Bardajee, *Heteroatom. Chem.*, 2006, **17**, 136–141.

- [77] R. Benn, A. Ruffńska, H. Lehmkuhl, E. Janssen and C. Krüger, *Angew. Chem., Int. Ed. Eng.*, 1983, **22**, 779–780. View Article Online
DOI: 10.1039/C7DT02435E
- [78] R. Benn and A. Ruffńska, *Angew. Chem., Int. Ed. Eng.*, 1986, **25**, 861–881.
- [79] D. A. Atwood and M. J. Harvey, *Chem. Rev.*, 2001, **101**, 37–52.
- [80] The τ value ranges from 0 (perfectly square planar) to 1 (perfectly trigonal tetrahedral). L. Yang, D. R. Powell and R. P. Houser, *Dalton Trans.*, 2007, 955–964.
- [81] The τ' value ranges from 0 (perfectly square planar) to 1 (perfectly trigonal tetrahedral). A. Okuniewski, D. Rosiak, J. Chojnacki and B. Becker, *Polyhedron*, 2015, **90**, 47–57.
- [82] C. E. Radzewich, M. P. Coles and R. F. Jordan, *J. Am. Chem. Soc.*, 1998, **120**, 9384–9385.
- [83] C. E. Radzewich, I. A. Guzei and R. F. Jordan, *J. Am. Chem. Soc.*, 1999, **121**, 8673–8674.
- [84] Z. Zhong, P. J. Dijkstra and J. Feijen, *Angew. Chem., Int. Ed.*, 2002, **41**, 4510–4513.
- [85] N. Iwasa, S. Katao, J. Liu, M. Fujiki, Y. Furukawa and K. Nomura, *Organometallics*, 2009, **28**, 2179–2187.
- [86] M. Shen, W. Zhang, K. Nomura and W.-H. Sun, *Dalton Trans.*, 2009, 9000–9009.
- [87] M. Shen, W. Huang, W. Zhang, X. Hao, W.-H. Sun and C. Redshaw, *Dalton Trans.*, 2010, **39**, 9912–9922.
- [88] The τ value ranges from 0 (perfectly square pyramidal) to 1 (perfectly trigonal bipyramidal). A. W. Addison, T. N. Rao, J. Reedijk, J. van Rijn and G. C. Verschoor, *J. Chem. Soc., Dalton Trans.*, 1984, 1349–1356.
- [89] M.-A. Munoz-Hernandez, T. S. Keizer, P. Wei, S. Parkin and D. A. Atwood, *Inorg. Chem.*, 2001, **40**, 6782–6787.

- [90] I. Barakat, Ph. Dubois, R. Jérôme and Ph. Teyssié, *J. Polym. Sci. A Polym. Chem.*, 1993, **31**, 505–514. View Article Online
DOI:10.1039/C7DT02435E
- [91] J. Baran, A. Duda, A. Kowalski, R. Szymanski and S. Penczek, *Macromol. Rapid Commun.* 1997, **18**, 325–333.
- [92] A. Kowalski, A. Duda and S. Penczek, *Macromolecules*, 1998, **31**, 2114–2122.
- [93] A. Amgoune, C. M. Thomas and J.-F. Carpentier, *Macromol. Rapid Commun.*, 2007, **28**, 693–697.
- [94] M. Helou, O. Miserque, J.-M. Brusson, J.-F. Carpentier and S. M. Guillaume, *Chem. Eur. J.* 2008, **14**, 8772–8775.
- [95] C. Guillaume, J.-F. Capentier and S. M. Guillaume, *Polymer*, 2009, **50**, 5909–5917.
- [96] N. Ajellal, J.-F. Carpentier, C. Guillaume, S. M. Guillaume, M. Helou, V. Poirier, Y. Sarazin and A. Trifonov, *Dalton Trans.* 2010, **39**, 8363–8376.
- [97] S. Qiao, W.-A. Ma and Z.-X. Wang, *J. Organomet. Chem.*, 2011, **696**, 2746–2753.
- [98] H.-J. Chuang, Y.-C. Su, B.-T. Ko and C.-C. Lin, *Inorg. Chem. Commun.*, 2012, **18**, 38–42.
- [99] K. D. Rebecca, A. M. Reckling, H. Chen, L. N. Dawe, C. M. Schneider and C. M. Kozak, *Dalton Trans.*, 2013, **42**, 3504–3520.
- [100] F. Hild, N. Neehaul, F. Bier, M. Wirsum, C. Gourlaouen and S. Dagorne, *Organometallics*, 2013, **32**, 587–598.
- [101] C.-H. Wang, C.-Y. Li, B.-H. Huang, C.-C. Lin and B.-T. Ko, *Dalton Trans.*, 2013, **42**, 10875–10884.
- [102] N. M. Rezayee, K. A. Gerling, A. L., Rheingold, Fritsch and J. M. *Dalton Trans.*, 2013, **42**, 5573–5586.
- [103] X.-F. Yu, C. Zhang and Z.-X. Wang, *Organometallics*, 2013, **32**, 3262–3268.
- [104] Z. Tang and V. C. Gibson, *Eur. Polym. J.*, 2007, **43**, 150–155.

- [105] J. Wu, Y.-Z. Chem, W.-C. Hung and C.-C. Lin, *Organometallics*, 2008, **27**, 4970–4978. Article Online DOI: 10.1039/C7DT02435E
- [106] K. Ding, M. O. Miranda, B. Moscata-Goodpaster, N. Ajellal, L. E. Breyfogle, E. D. Hermes, C. P. Schaller, S. E. Roe, C. J. Cramer, M. A. Hillmyer and W. B. Tolman, *Macromolecules*, 2012, **45**, 5368–5396.
- [107] S. Bian, S. Abbina, Z. Lu, E. Kolodka and G. Du, *Organometallics*, 2014, **33**, 2489–2495.
- [108] L. M. Alcazar-Roman, B. J. O’Keefe, M. A. Hillmyer and W. B. Tolman, *Dalton Trans.*, 2003, 3082–3087.
- [109] K. A. M. Thakur, R. T. Kean, E. S. Hall, J. J. Kolstad, T.A. Lindgren, M. A. Doscotch, J. I. Siepmann and E. J. Munson, *Macromolecules*, 1997, **30**, 2422–2428.
- [110] J. Coudane, C. Ustariz-Peyret, G. Schwach and M. Vert, *J. Poly. Sci. A Polym. Chem.*, 1997, **35**, 1651–1658.
- [111] K. A. M. Thakur, R. T. Kean, E. S. Hall, J. J. Kolstad and E. J. Munson, *Macromolecules*, 1998, **31**, 1487–1494.
- [112] K. A. M. Thakur, R. T. Kean, M. T. Zell, B. E. Padden and E. J. Munson, *Chem. Commun.*, 1998, 1913–1914.
- [113] M. H. Chisholm, S. S. Iyer, D. G. McCollum, M. Pagel and U. Werner-Zwanziger, *Macromolecules*, 1999, **32**, 963–973.
- [114] M. T. Zell, B. E. Padden, A. J. Paterick, K. A. M. Thakur, R. T. Kean, M. Hillmyer and E. J. Munson, *Macromolecules*, 2002, **35**, 7700–7707.
- [115] M. Lamberi, I. D’Auria, M. Mazzeo, S. Milione, V. Bertolasi and D. Pappalardo, *Organometallics*, 2013, **31**, 5551–5560.
- [116] J. S. Klitzke, T. Roisnel, E. Kirillov, O. de L. Casagrande Jr and J.-F. Carpentier, *Organometallics*, 2013, **33**, 5693–5707.

- [117] E. L. Marshall, V. C. Gibson and H. S. A. Rzepa, *J. Am. Chem. Soc.*, 2005, **127**, 6048–6051. View Article Online
DOI: 10.1039/C5DT02435E
- [118] A. P. Dove, V. C. Gibson, E. L. Marshall, H. S. Rzepa, A. J. P. White and C. K. Williams, *J. Am. Chem. Soc.*, 2006, **128**, 9834–9843.
- [119] N. Barros, P. Mountford, S. M. Guillaume and L. Maron, *Chem. Eur. J.*, 2008, **14**, 5507–5518.
- [120] J. Börner, I. dos Santos Vieira, A. Pawlis, A. Döring, D. Kuckling and S. Herres-Pawlis, *Chem. Eur. J.*, 2011, **17**, 4507–4512.
- [121] J. Fang, I. Yu, P. Mehrkhodavandi and L. Maron, *Organometallics*, 2013, **32**, 6950–6956.
- [122] L. Wang, C. E. Kefalidis, S. Sinbandhit, V. Dorcet, J.-F. Carpentier, L. Maron and Y. Sarazin, *Chem. Eur. J.*, 2013, **19**, 13463–13478.
- [123] M. O. Miranda, Y. DePorre, H. Vazquez-Lima, M. A. Johnson, D. J. Marell, C. J. Cremer and W. B. Tolman, *Inorg. Chem.*, 2013, **52**, 13692–13701.
- [124] F. D. Monica, E. Luciano, G. Roviello, A. Grassi, S. Milione and C. Capacchione, *Macromolecules*, 2014, **47**, 2830–2841.
- [125] D. Jędrzkiewicz, D. Kantorska, J. Wojtaszak, J. Ejfler and S. Szafert, *Dalton Trans.*, 2017, **46**, 4249–4942.
- [126] J. Wei, M. N. Riffel and P. L. Diaconescu, *Macromolecules*, 2017, **50**, 1847–1861.
- [127] C. Robert, T. E. Schmid, V. P. Richard, Haquette, S. K. Raman, M.-N. Rager, R. M. Gauvin, Y. Morin, X. Trivelli, V. Guérineau, I. del Rosal, L. Maron and C. M. Thomas, *J. Am. Chem. Soc.*, 2017, **139**, 6217–6225.
- [128] M. J. Frisch, G. W. Trucks, H. B. Schlegel, G. E. Scuseria, M. A. Robb, J. R. Cheeseman, G. Scalmani, V. Barone, B. Mennucci, G. A. Petersson, H. Nakatsuji, M. Caricato, X. Li, H. P. Hratchian, A. F. Izmaylov, J. Bloino, G. Zheng, J. L.

Sonnenberg, M. Hada, M. Ehara, K. Toyota, R. Fukuda, J. Hasegawa, M. Ishida, T. Nakajima, Y. Honda, O. Kitao, H. Nakai, T. Vreven, J. A. Montgomery, Jr, J. E. Peralta, F. Ogliaro, M. Bearpark, J. J. Heyd, E. Brothers, K. N. Kudin, V. N. Staroverov, R. Kobayashi, J. Normand, K. Raghavachari, A. Rendell, J. C. Burant, S. S. Iyengar, J. Tomasi, M. Cossi, N. Rega, J. M. Millam, M. Klene, J. E. Knox, J. B. Cross, V. Bakken, C. Adamo, J. Jaramillo, R. Gomperts, R. E. Stratmann, O. Yazyev, A. J. Austin, R. Cammi, C. Pomelli, J. W. Ochterski, R. L. Martin, K. Morokuma, V. G. Zakrzewski, G. A. Voth, P. Salvador, J. J. Dannenberg, S. Dapprich, A. D. Daniels, Ö. Farkas, J. B. Foresman, J. V. Ortiz, J. Cioslowski and D. J. Fox, *Gaussian 09*, revision D.01; Gaussian, Inc.: Wallingford, CT, 2009.

- [129] U. Zhao and D. G. Truhlar, *J. Chem. Phys.*, 2006, **125**, 1–17.
- [130] Y. Zhao and D. G. Truhlar, *Theor. Chem. Acc.*, 2008, **120**, 215–241.
- [131] Y. Zhao and D. G. Truhlar, *Acc. Chem. Res.*, 2008, **41**, 157–167.
- [132] W. J. Hehre, R. Ditchfield and J. A. Pople, *J. Chem. Phys.*, 1972, **56**, 2257–2261.
- [133] S. Matsui, M. Mitani, J. Saito, Y. Tohi, H. Makio, N. Matsukuwa, Y. Takagi, K. Tsuru, M. Nitabaru, T. Nakano, H. Tanaka, N. Kashiwa and T.A. Fujita, *J. Am. Chem. Soc.*, 2001, **123**, 6847–6856.
- [134] H. E. Gottlieb, B. Kotlyar and A. Nudelman, *J. Org. Chem.*, 1997, **62**, 7512–7515.
- [135] Bruker (2015). APEX3 and SAINT. Bruker–Nonius AXS Inc., Madison, Wisconsin, USA.
- [136] L. Krause, R. Herbst-Irmer, G. M. Sheldrick and D. Stalke, *J. Appl. Cryst.* 2015, **48**, 3–10.
- [137] O.V. Dolomanov, L. J. Bourhis, R. J. Gildea, J. A. K. Howard and H. Puschmann, *J. Appl. Cryst.*, 2009, **42**, 339–341.
- [138] G. M. Sheldrick, *Acta Cryst.*, 2015, **A71**, 3–8.

- [139] C. F. Macrae, P.R. Edgington, P. McCabe, E. Pidcock, G. P. Shields, R. Taylor, M. Towler and J. van de Streek, *J. Appl. Cryst.*, 2006, **39**, 453–457. View Article Online
DOI: 10.1039/C7DT02435E